On the Use of Ultrasound Phase Data for Arterial Characterization

Erlöv, Tobias

2015

Total number of authors:
1

On the use of ultrasound phase data for arterial characterization

Tobias Erlöv

LUND UNIVERSITY

Organization: Lund University Department of Biomedical Engineering P.O. Box 118, SE-221 00 Lund, Sweden	Document name: Doctoral Dissertation
	Date of issue: September 25, 2015
	Sponsoring organization: Innovative Medicines Initiative, European Commission Research and Innovation, Swedish Foundation for International Cooperation in Research and Higher Education, Swedish Research Council
Author: Tobias Erlöv	

Title: On the use of ultrasound phase data for arterial characterization

Abstract:

Atherosclerosis is one of the major causes of death in the world. It is an inflammatory disease in the arteries which causes a gradual increase in arterial wall thickness and stiffness. Eventually a plaque could be formed, protruding into the artery and partially occluding the blood flow. Rupture of such a plaque could cause cardiac infarction or stroke. This dissertation revolves around finding better methods to detect and diagnose different stages of atherosclerosis and also to better understand the physiology of arteries. The methods developed and presented in this dissertation are all based on non-invasive ultrasound images. Ultrasound is the most common tool to image, particularly, the carotid artery in clinics today.

The first method utilizes the time domain phase of the ultrasound radio frequency data for plaque/tissue characterization. The center frequency of the backscattered signal is estimated using phase differences measured in the time domain. We have shown that there is a clear correlation between the center frequency shift (CFS) and scatter size using a series of agar phantoms with well-defined sizes of glass beads. We have also shown that the CFS can be used *in vivo* to determine carotid plaque vulnerability. The method could potentially become a useful tool to identify patients at risk for development of acute cardiovascular events as well as to monitor response to interventions. The second and third methods are based on motion tracking (one is again based on time domain phase data) and could be used to measure e.g. the longitudinal movement of the arterial wall. The longitudinal movement is a relatively recent discovered physiological phenomena and could potentially be used as an image-derived biomarker for vascular dysfunction. Measurements of the longitudinal movement are also interesting from a physiological point of view since the mechanism behind it is unclear. The fourth and fifth methods measure the thickness and diameter of the arterial wall during the cardiac cycle. Arterial wall thickness measurements are a standard procedure in cardiovascular research and may be used for early diagnosis of atherosclerosis. Although there is a large number of automatic methods developed for this purpose, most of these measurements are still made manually. One of our methods is the first to automatically measure the thickness and diameter of arteries in a small animal model.

Keywords: Atherosclerosis, Ultrasound, Carotid Artery, Plaque Characterization, Scatter Size, Longitudinal Movement, Intima-Media Thickness

Classification system and/or index terms:

Supplementary bibliographical information: ISRN LUTEDX/TEEM - 1097 – SE, Report 1/15	Language: English
ISSN and key title:	ISBN: 978-91-7623-452-5 (Print) 978-91-7623-453-2 (Electronic)
Recipient´s notes:	Number of pages: 148	Price:
	Security classification:	

Signature: _[signature]_   Date: 2015-08-25

To my parents

Nothing is impossible, the word itself says "I'm possible"!

Audrey Hepburn

Cover illustration
Schematic illustration of an ultrasound examination of the carotid artery and images obtained from two different arterial characterization methods (Papers II and III).

Public defence
Sep 25, 2015, 10.15 in E:1406, E-huset, Faculty of Engineering, LTH

Advisors
Associate Professor Magnus Cinthio
Professor Hans W Persson
Associate Professor Tomas Jansson
Associate Professor Isabel Gonçalves
Professor Jan Nilsson
Associate Professor Åsa Rydén Ahlgren
Lund University, Sweden

Faculty Opponent
Professor Elisa Konofagou
Department of Biomedical Engineering, Columbia University, New York, NY, USA
Department of Radiology, Columbia University, New York, NY, USA

Board of Examination
Professor Karl Åström
Centre for Mathematical Sciences, Faculty of Engineering, LTH, Lund University, Sweden
Professor Tino Ebbers
Department of Medical and Health Sciences, Linköping University, Sweden
Associate Professor Matilda Larsson
Technology and Health, Royal Institute of Technology, Stockholm, Sweden
Deputy member: Associate Professor Sven Månsson
Medical Radiation Physics, Malmö, Lund University, Sweden

Chairman
Associate Professor Johan Nilsson
Department of Biomedical Engineering, Faculty of Engineering, LTH, Lund University, Sweden

PREFACE

The PhD studies have gone so fast! Yet, a lot has happened during these years and a lot of work has been done. I would like to start with an acknowledgment to all of those who have contributed and helped me in the work of this dissertation.

First of all I would like to thank Magnus Cinthio for being such a great supervisor, for your never-ending support, encouragement and for trusting me to explore new grounds. You have really helped me to balance my way forward, lending me a hand whenever needed. Special thanks also to Tomas Jansson and Hans W Persson for all valuable inputs and the countless, interesting, hopeless, hopeful and fun meetings. Magnus Cinthio, Tomas Jansson, Monica Almqvist, Hans W Persson and Kjell Lindström: I really appreciate your friendliness, your openness and also your efforts in the graduate courses. You are the reason I chose biomedical engineering!

Many thanks also to Isabel Gonçalves for all your hard work and commitment and for always being so happy and positive. I miss the intense (and crowded) weeks in your office! To Jan Nilsson for your enthusiastic drive forward and for your valuable perspectives. To Åsa Rydén Ahlgren for inviting me with open arms to the world of arteries. You inspire me with your sincere interest in physiology and I am happy for all of your thorough reviews. I would also like thank Simon Segstedt for all of the fun work we did together. It was a great time and I hope we team up again soon! To Maria Evertsson and John Albinsson for being such great and close colleagues during all years at the department! I have really enjoyed the time at the office and all the conferences we have been at together! Thanks also to Roger Andersson and Mattias Holmer, especially for keeping me company during this vacationless summer! And of course I would also like to thank all other colleagues at the department for all lunch- and coffee- (or rather tea) break discussions and for creating such nice atmosphere at work.

Many thanks to Mats Hansson for a thorough review of the dissertation, for all deep (and other ;)) discussions, for always being slightly better than me at table tennis and above all for being such a good friend! Warm thanks to my beloved parents and siblings for always being there (and for being so refreshingly non-academic). And finally, I would like to thank my wife and children for everything, you have my heart!

POPULÄRVETENSKAPLIG SAMMANFATTNING

Hjärt- och kärlsjukdomar som till exempel åderförkalkning utgör en av världens vanligaste dödsorsaker. I den här avhandlingen har vi utvecklat olika metoder som med hjälp av bildanalys ger värdefull information om kärlväggen i syfte att förbättra kunskapen om artärer och framförallt åderförkalkning. I avhandlingen presenteras fem olika metoder som alla är baserade på bilder som är tagna med hjälp av ultraljud. Tillsammans möjliggör dessa metoder nya och säkrare sätt att diagnostisera olika skeden av åderförkalkning. Till exempel har vi visat att en av metoderna kan användas för att karaktärisera arteriella plack, vilket kan innebära en säkrare bedömning om en patient riskerar att drabbas av stroke eller hjärtinfarkt.

Åderförkalkning innebär att kärlen i kroppen blir allt stelare. Bindväv, fett och inflammatoriska partiklar samlas i kärlväggarna som blir gradvis tjockare. En lokal större ansamling av till exempel fett och inflammatoriska partiklar kallas för ett arteriellt plack. Plack kan vara så stora att de trycker in kärlväggen i blodbanan och hindrar blodflödet. Det finns alltid en risk att kärlväggen runt ett plack spricker. När detta händer börjar blodet koagulera och det bildas en propp. Detta innebär en akut kärlkomplikation där blodflödet stoppas och efterliggande vävnad snabbt lider av syrebrist. Hjärtinfarkt (propp i hjärtat) och stroke (propp i hjärnan) är två vanliga följder. Hur stor risken är att ett plack brister beror till stor del på plackets innehåll. Plack med en stor kärna av fett och inflammerade celler innebär en stor risk medan ett plack med mycket bindväv utgör en mindre risk. Idag saknas effektiva verktyg i både sjukvård och medicinsk forskning för att på ett optimalt sätt diagnostisera graden av åderförkalkning, både i tidiga och sena skeden. Det finns idag inget effektivt sätt att i förväg se om ett arteriellt plack är farligt (har stor risk att brista) eller inte, vilket hade varit önskvärt vid till exempel bedömning om en patient ska opereras eller inte.

Syftet med den första metoden (presenteras i artikel I och II) är att ta fram ett mått i ultraljudsignalen som är vävnadsberoende och som därmed kan användas för att bedöma om arteriella plack är farliga eller inte. En enda ultraljudspuls innehåller många olika frekvenser och när ljudet reflekteras fördelas dessa frekvenser olika beroende på vilken vävnad det är. Till exempel kan storleken på vävnadens reflekterande strukturer spela en betydande roll. Med denna metod mäter vi frekvens i tidsdomänen vilket innebär att vi endast mäter medelfrekvensen, fast med högre noggrannhet och bättre upplösning jämfört med andra metoder, så kallade spektralmetoder. I den ena artikeln utvärderar vi hur vår uppmätta frekvens relaterar till just storleken på spridarna (reflekterande strukturer/objekt) med hjälp av fantomer, alltså konstgjorda material som liknar mänsklig vävnad. Resultatet visade ett starkt samband som också väl följde den teoretiska modell vi använde. I den andra artikeln

testar vi metoden på mänskliga plack i halspulsådern. Det visade sig finnas ett starkt samband mellan resultatet från metoden och hur farliga placken var. Metoden har därför potential att ge en säkrare bedömning om en patient riskerar att drabbas av stroke eller hjärtinfarkt.

Två av de andra metoderna (presenteras i artikel III och VII) baseras på rörelsemätning. Sådana metoder är användbara för att mäta vävnadsegenskaper som till exempel elasticitet men även förekomsten av en rörelse och storleken på den kan vara av stort intresse, både inom fysiologisk och patofysiologisk forskning. Den ena metoden är en generell rörelsemätningsmetod som på ett unikt och mycket snabbt sätt beräknar rörelsen i ultraljudsbilder. Den andra metoden är speciellt utformad för att mäta den longitudinella rörelsen (längs med blodflödet) i kärlväggen. Den longitudinella rörelsen och den skjuvning som uppstår inuti väggen har upptäckts och undersökts först under de senaste tio åren, först av vår forskargrupp men senare även av ett flertal andra. Syftet med just denna metod var att för första gången mäta den kontinuerliga fördelningen av skjuvningen. Resultatet visade att en mycket stor del av skjuvningen sker i övergången mellan kärlväggens två yttre lager, något som kan vara av stort intresse inom den fysiologiska forskningen.

De resterande två metoderna (presenteras i artiklarna IV, V och VI) mäter med hjälp av segmentering väggtjockleken och diametern på blodkärl och hur dessa varierar under ett hjärtslag. Syftet är att på ett snabbt och automatiskt sätt (ofta utvärderas många tusen patienter) ge kunskap om tidiga förändringar i kärlväggens dimensioner och elasticitet på grund av åderförkalkning. Vår metod kan användas för mätningar på till exempel halspulsådern men är också den första metoden som samtidigt och automatiskt kan mäta både diameter och tjocklek på artärer i små djur.

LIST OF PUBLICATIONS

Included

I. **Scatter size estimation using the center frequency assessed from ultrasound time domain data.**
Tobias Erlöv, Tomas Jansson, Hans W Persson and Magnus Cinthio
Submitted

Author's contribution: All method development, phantom manufacturing, analysis and writing of first draft. Major part of study design.

II. **Determining carotid plaque vulnerability using ultrasound center frequency shifts.**
Tobias Erlöv, Magnus Cinthio, Andreas Edsfeldt, Simon Segstedt, Nuno Dias, Jan Nilsson and Isabel Gonçalves
Submitted

Author's contribution: All method development. Large part of analysis and writing

III. **A fast 2D tissue motion estimator based on the phase of the intensity enables visualization of the propagation of the longitudinal movement in the carotid artery wall.**
Tobias Nilsson, Åsa Rydén Ahlgren, John Albinsson, Simon Segstedt, Jan Nilsson, Tomas Jansson, Hans W Persson and Magnus Cinthio
Proceedings of the IEEE International Ultrasonics Symposium. Prague. 2013: 1761-1764.

Author's contribution: All method development and analysis and writing of first draft.

IV. **Automatic measurements of diameter, distension and intima media thickness of the aorta in premature rabbit pups using B-Mode images.**
Tobias Nilsson, Simon Segstedt, Patrik Milton, Snjolaug Sveinsdottir, Tomas Jansson, Hans W. Persson, David Ley and Magnus Cinthio
Ultrasound in medicine & biology 2014 Feb; 40(2): 371-7, 2014

Author's contribution: Large part of method development, analysis and writing.

V.   **A robust and fast method for arterial lumen diameter and intima-media thickness measurements.**
<u>Tobias Nilsson</u>, Simon Segstedt, Åsa Rydén Ahlgren, Stefano Ricci, Gerd Östling, Piero Tortoli, Jan Nilsson, Tomas Jansson, Hans W Persson and Magnus Cinthio
Proceedings of the IEEE International Ultrasonics Symposium. Dresden. 2012: 1678-1681.

Author's contribution: Large part of method development, study design, analysis and writing.

VI.   **A method for measuring the variation of intima-media thickness during the entire cardiac cycle using B-Mode images.**
<u>Tobias Nilsson</u>, Åsa Rydén Ahlgren, Tomas Jansson, Hans W Persson, Kjell Lindström, Jan Nilsson and Magnus Cinthio
Proceedings of the IEEE International Ultrasonics Symposium. Orlando. 2011: 2126-2129.

Author's contribution: All method development and analysis. Major part of study design and writing.

VII.   **A method to measure shear strain with high spatial resolution in the arterial wall non-invasively *in vivo* by tracking zero-crossings of B-Mode intensity gradients.**
<u>Tobias Nilsson</u>, Åsa Rydén Ahlgren, Tomas Jansson, Hans W Persson, Kjell Lindström, Jan Nilsson and Magnus Cinthio
Proceedings of the IEEE International Ultrasonics Symposium. San Diego. 2010: 491-494.

Author's contribution: All method development and analysis. Major part of study design and writing.

Related

Longitudinal displacement and intramural shear strain of the porcine carotid artery undergo profound changes in response to catecholamines.
Åsa Rydén Ahlgren, Magnus Cinthio, Stig Steen, Tobias Nilsson, Trygve Sjöberg, Hans W Persson and Kjell Lindström
American Journal of Physiology - Heart Circulation Physiology 302: H1102-H1115, 2012

Profound increase in longitudinal displacements of the porcine carotid artery wall can take place independently of wall shear stress: A continuation report.
Åsa Rydén Ahlgren, Stig Steen, Simon Segstedt, Tobias Erlöv, Kjell Lindström, Trygve Sjöberg, Hans W Persson, Stefano Ricci, Piero Tortoli and Magnus Cinthio
Ultrasound in medicine & biology 2015 Feb pp1-12 2015.

Methods for measurements of the longitudinal movement and the shear-induced longitudinal elastic modulus of the arterial wall.
Tobias Nilsson, Stefano Ricci, Åsa Rydén Ahlgren, Tomas Jansson, Kjell Lindström, Piero Tortoli, Hans W Persson and Magnus Cinthio
Proceedings of the IEEE International Ultrasonics Symposium. Rome. 2009: 317-320.

CONTENTS

1. INTRODUCTION

Every year more people die from cardiovascular diseases than from any other cause. With an estimated loss of 17.3 million people annually this constitutes 30% of all global deaths.[1] In most of these cases atherosclerosis is the underlying cause with subsequent cardiovascular events such as cardiac infarction and stroke. There is an extensive ongoing research to better understand the pathophysiological process and to detect and treat patients earlier and more efficiently. Unfortunately the cause and progress of atherosclerosis is very complex and not easily understood and a great deal of research still remains before this disease can be effectively assessed. The papers in this dissertation revolve around finding imaging methods to detect and diagnose different stages of atherosclerosis and also to enable better understanding of the physiology of arteries.

Ultrasound imaging is an easy, harmless, cheap and in many ways excellent technique for visualizing internal structures of the body. It is also the tool of choice for routine examinations of the carotid artery (the artery in the neck) and it is not unusual that this is the site where atherosclerosis is first detected. The methods developed and presented in this dissertation are all based on image analysis and signal processing of ultrasound images.

1.1 Outline

The outline of this dissertation will be as follows: First, the pathophysiological process and basic understanding of atherosclerosis will be introduced. Then the concept of ultrasound is described, how it works, how it can be used and why it is used. The two subjects will then be combined in a larger chapter introducing arterial characterization using ultrasound. This chapter will be divided into several parts each describing different technical approaches, both in what they measure and how. It is important to note that there cannot be a single optimal solution that will answer all questions and solve everything. Different aspects or stages of atherosclerosis pose different questions and clinical needs and must therefore be assessed in different ways. Finally, there is a short introduction to each of the included papers followed by the actual papers.

2.   ATHEROSCLEROSIS

The general description of atherosclerosis given in this section is regarded as widely accepted in this field of research. Much of the material (and a more elaborate description) is given in an excellent review article by Ross[2] and in the book *McDonald's Blood Flow in Arteries*[3] unless otherwise stated.

Atherosclerosis is an inflammatory disease which mainly occur in large to medium-sized arteries. It is the primary cause of death in Europe, United States and much of Asia. Figure 1 shows the anatomy of a large to medium-sized artery. The arterial wall can be divided into three different layer; *tunica intima*, *tunica media* and *tunica externa*. Tunica intima or simply *intima*, is a rather thin layer of endothelial cells which are in direct contact with the blood stream. The endothelial cells are followed by an elastic tissue called internal elastic lamina which connects the intima to the middle layer. The middle layer, tunica media or simply *media*, is composed of transversally arranged smooth muscle cells and connective tissue. There is also an elastic tissue connecting the media to the outer layer and this is called the external elastic lamina. The media varies in thickness depending on the size of the artery and is usually the thickest layer. The artery is bound to the surrounding tissue by its outer layer, tunica externa or more commonly *adventitia*, containing collagen fibers.

The development of atherosclerosis is lately recognized as a response to injury of the arterial wall. Common risk factors for developing atherosclerosis include smoking, high amounts of certain fats and cholesterols in the blood, high blood pressure, diabetes and obesity.[4] An injury to the intima leads to an inflammatory response with
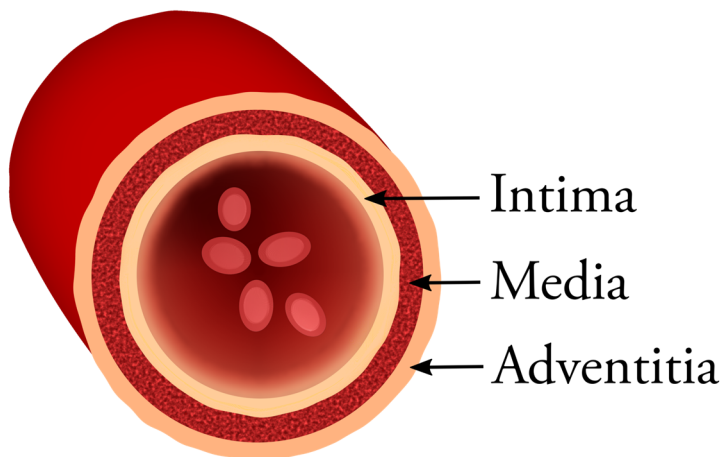

Figure 1. A schematic cross section of an artery. From within, the arterial wall consists of three layers: intima, media and adventitia.

increased adhesiveness of the endothelium which attracts leukocytes (white blood cells) and platelets. Cytokines and growth factors are released which stimulates cellular growth and differentiation. This is a normal inflammatory response to heal the injury. However, if this response fail to eliminate the cause of injury it will continue indefinitely causing an inflammatory disorder which may in itself result in more advanced and complicated lesions.

Inflammatory mediators such as the macrophage colony-stimulating factor stimulates the formation of lipid-laden macrophages, so-called foam cells. These foam cells accumulate in the intima forming fatty streaks. An unrestricted inflammatory response will stimulate smooth muscle cells to migrate from the media into the intima where they proliferate (increase in number) and cause what is called an intermediate-lesion. This process thickens the arterial wall. Lymphocytes and a specific type of white blood cells called monocytes accumulate in the area of inflammation where the latter differentiate into macrophages. When lymphocytes and macrophages are activated they release more cytokines and growth factors. This causes a spiral where more smooth muscle cells migrate, proliferate and form fibrous tissue with further enlargement of the wall – an atherosclerotic *plaque* is formed. The inflammation leads to tissue damage and ultimately necrosis (tissue death). Eventually fibrous tissue surrounds a gradually growing necrotic core. The plaque intrudes into the artery partially (or completely) blocking the blood flow (see Fig. 2).
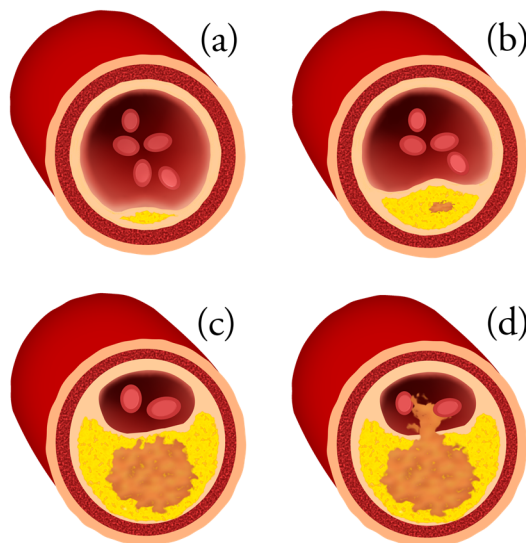

Figure 2. Gradually growing atherosclerotic plaque (a-c) where finally d) the fibrous cap separating a necrotic core from the blood ruptures and various debris leaks into the blood stream.

The growing necrotic core gradually thins the fibrous cap which separates it from the blood flow. If the fibrous cap ruptures it releases various debris into the blood stream. This rupture attracts platelets and leads to the formation of thrombus which further blocks the blood flow, either at the site of the rupture or further downstream. Such blockage often causes cardiac infarction (if in the coronary arteries) or stroke (if in the cerebral arteries).

Several studies[5-8] have shown that there is a link between blood flow alterations and plaque formation. Curvatures such as arterial branches and bifurcations induces alterations and turbulence in the blood flow. These sites are prone to form specific molecules on the endothelium which are responsible for the increased adhesiveness and the onset of an inflammatory response. Reduced shear stress caused by the blood flow can increase the expression of several genes involved in the atherosclerotic process. Therefore, it appears that alterations in the blood flow, the amount of shear stress and turbulence at a specific region of an artery, is a vital tool to predict whether that region is prone to have lesions.

Unfortunately, symptoms of atherosclerosis often do not appear until there is a cardiovascular event causing a medical emergency, such as a heart attack or stroke. A common symptom is angina (chest pain) if the blockage is in the heart. This occurs when the heart muscle does not get enough oxygen. If the blockage is in the brain symptoms are that of a stroke, e.g. sudden weakness, paralysis (especially on one side of the body), speech difficulty, visual disturbance and sudden and severe headache.

Cardiovascular diseases such as atherosclerosis also constitute a heavy economic burden. In 2010 the estimated direct and indirect cost of coronary heart disease and stroke alone in the US was more than $160 billion. In 2030 the direct costs are projected to triple and the indirect costs to increase with almost two thirds.[9] Figure 3 shows an atherosclerotic plaque surgically removed from a human carotid artery.
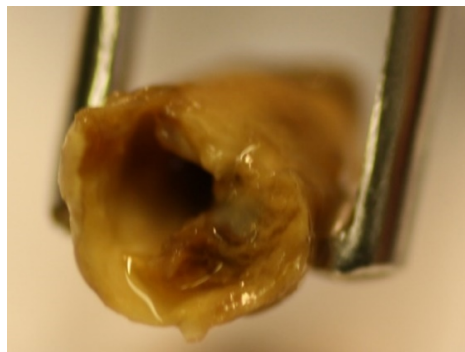
Figure 3. Surgically excised human carotid plaque.
(Photo by Andreas Edsfeldt)

3.   ULTRASOUND

3.1   Theory

Sound waves are mechanical waves that propagate though a medium. Each material has a specific density and compressibility which together determine the speed of sound and the acoustic impedance of that material. The acoustic impedance is an important parameter to consider in order to predict how the sound behaves when it enters a heterogeneous medium. A heterogeneous medium consists of several different materials, each with their own acoustic impedance. When a sound wave encounters a boundary between two materials with different acoustic impedance the wave partially reflects. The ratio of the reflected energy to the transmitted energy is determined by how large this difference is.

A source that emits a sound pulse towards such a boundary will, due to the reflection, receive an echo after a certain time (see Fig. 4). The time interval between the pulse transmission and echo-arrival is determined by the speed of sound and the distance between the source and the boundary. This "pulse-echo" effect is the fundamental principal in a large number of applications including the medical ultrasound scanner. Bats and dolphins use the pulse-echo technique for navigation and to locate their prey. Marine vessels use sound navigation and ranging (SONAR) to scan the sea floor or to locate schools of fish, and modern cars often have parking sensors, both utilize the pulse-echo technique.
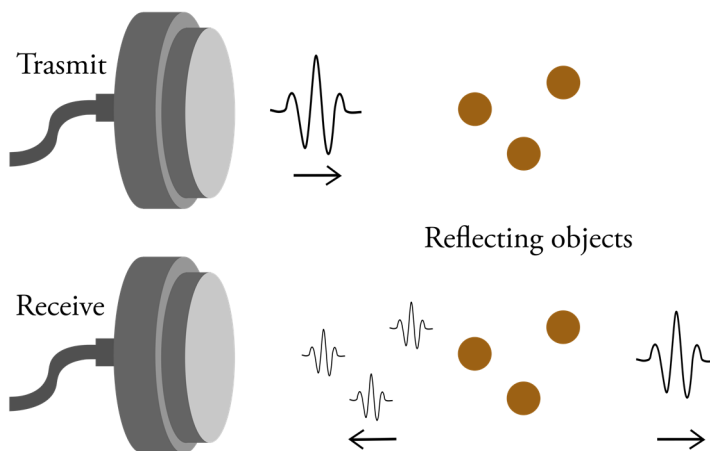
Figure 4. The "pulse-echo" principle. A pulse is transmitted towards an area of interest and is then reflected from one or several scattering objects. If the acoustic impedance of the scattering objects are similar to that of the surrounding medium, the echoes are rather weak and most of the energy will remain in the original pulse.

A common feature for the applications above is the use of ultrasound. Ultrasound is sound with a frequency above 20 kHz, i.e. sound that is inaudible to the human ear. The benefit of using such high frequencies is that the origin of the echoes can be determined with higher resolution. On the other hand higher frequencies will be attenuated more quickly. Therefore, there is usually a trade-off between resolution and how far the sound can travel.

A medical ultrasound scanner usually transmits ultrasound pulses with frequencies between 2-15MHz depending on the depth of the tissue being investigated. A transmitted pulse is reflected at all underlying tissue interfaces (changes in acoustic impedance). The ultrasound scanner then measures the arrival time of the returning echoes and by knowing the speed of sound the origin of the echoes can be determined. The ultrasound raw data is called radio frequency (RF) data and reflects the oscillating sound pressure on the transducer surface. One transmitted pulse yields an 1D image or a so called A-line. If several subsequent pulses are transmitted adjacent to each other,
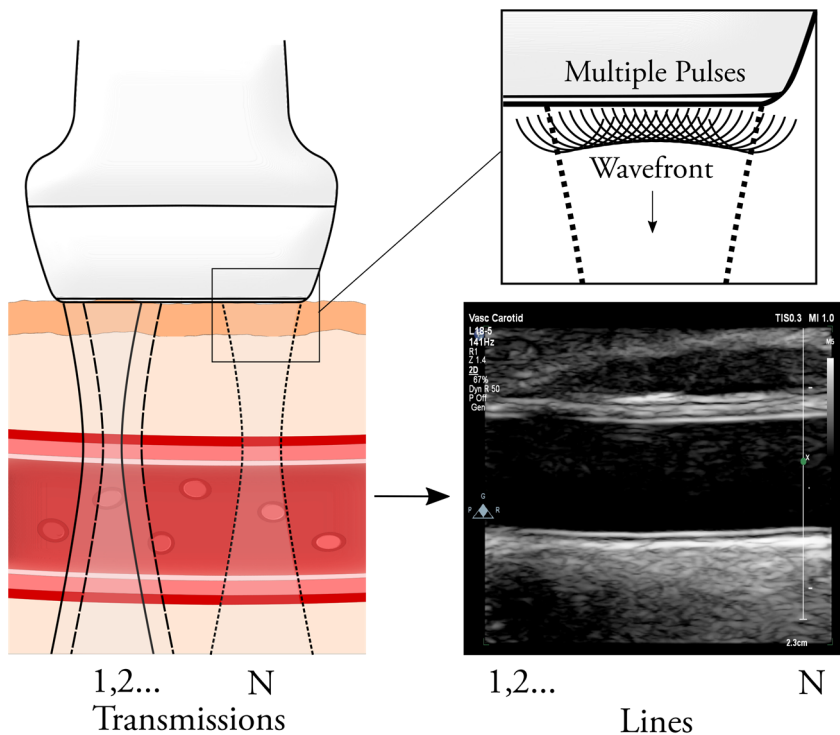
Figure 5. A schematic illustration of how a standard B-Mode image is created. Each B-Mode line corresponds to one ultrasound transmission. Each ultrasound transmission (made by pulses from several piezoelectric elements) results in a wavefront whose shape and direction depends on the time delays of all pulses used to create it. The amplitude of a returning echo determines the image brightness at the corresponding location, where white means high amplitude.

a 2D image can be formed. In 2D images, called B-Mode images, the brightness reflects the intensity of the sound. Boundaries with large difference in acoustic impedance cause more energy to be reflected and will thereby be depicted more brightly. Figure 5 show the principle of how standard B-Mode images are created. Each line in the B-Mode image corresponds to the combined transmission of several elements (usually piezoelectric). The time delays between transmissions of these elements will shape the resulting wavefront and could be used to direct the "beam" or create a focus. The transducer then awaits the returning echoes and repeats the process for the next line, but with another set of elements.

It is also common to measure velocity with ultrasound (see Fig. 6). This is referred to as Doppler measurements. The Doppler effect is the term for the phenomena where the frequency of a received sound changes depending on the relative velocity between the transmitter and the receiver. However, in medical ultrasound, which usually transmits pulses rather than continuous waves, the term Doppler is actually misleading. To measure blood flow velocity an ultrasound scanner transmits a series of pulses. When each ultrasound pulse reaches the blood vessel the red blood cells have moved a certain distance compared to the previous pulse, due to the flow velocity. This causes a translational change in the backscattered (reflected) ultrasound which is detected using appropriate signal processing. In other words, the blood flow velocity is basically determined by measuring the time lag in the backscattered data between adjacent pulses, rather than a change in frequency.
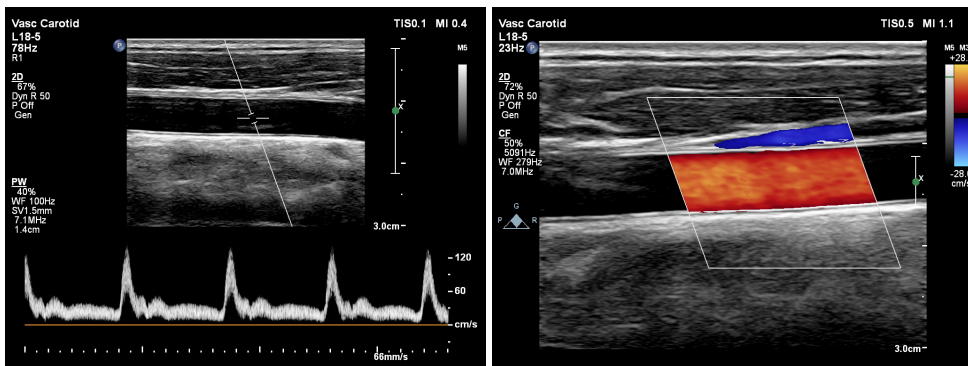

Figure 6. Velocity measurements using ultrasound. Left – pulsed Doppler is used to display all velocity (spectral) components versus time within a user-defined region. Right – color Doppler is used to display the current mean velocity within a larger area using color-coding.

3.2   Ultrasound in comparison to other imaging modalities

Ultrasound is only one out of several imaging modalities available in clinics today. This section aims to briefly introduce and to highlight the benefits and drawbacks of these modalities and to show when and why ultrasound is preferable to other techniques. A more elaborate introduction (in Swedish) to different medical imaging modalities is presented by Berglund and Jönsson[10].

3.2.1   Other imaging modalities

X-ray and Computed Tomography (CT)

An X-ray is a form of electromagnetic radiation created when electrons collide with a material with a high atomic number. The absorption (photoelectric absorption) of X-rays is basically determined by the density of the medium. Bones have a high density compared to surrounding tissue and are therefore clearly visible on medical X-ray images. Computed tomography, or commonly CT, is a technique where several X-ray images are combined to form a detailed tomographic image of the scanned area. X-ray images and CT scans have very high spatial resolution and are well suited for bone, lung and chest imaging and also cancer detection. Some applications involve injection of radio-opaque contrast agents. One such common application is coronary angiography which images the blood vessels in the heart. The injection of a contrast agent allows visualization of the presence and width of arteries. The narrowing caused by atherosclerotic plaques can thus be localized. A clear drawback with X-ray imaging and CT scans is that the radiation is ionizing (could ionize atoms and disrupt molecular bonds) meaning that it is harmful for living tissue.

Magnetic Resonance Imaging (MRI)

Magnetic Resonance Imaging (MRI) is a technique utilizing the high amount of water in the body. The hydrogen atoms are exposed to a strong magnetic field and if excited by a radio frequency wave the atoms precess (spin) orthogonally to the strong magnetic field and emit a detectable signal to the MRI scanner. By applying gradients in the magnetic field the scanner can control at which location and with which frequency hydrogen atoms precess. The scanner then interprets signal from different locations and forms an image. The material surrounding the hydrogen atom (different tissue) will determine how fast the atoms spin out of phase with the magnetic field and how much time is required for the atoms to return to their equilibrium state in the magnetic

field. This is used to differentiate tissue. Different contrast agents can be injected to enhance the contrast of a specific type of tissue. MRI scanners can, similarly to CT, produce three dimensional images but is best suited for soft tissue examination. MRI can also be used to image physiological function (fMRI). The spatial resolution is lower than that of CT but MRI has much more soft tissue details and has the benefit of not utilizing any ionizing radiation. The technique is considered safe for living tissue, however some patients show allergic reactions to the contrast dye. Other drawbacks include possible claustrophobia, long examination times and high examination costs.

Positron Emission Tomography (PET) and Single Photon Emission Tomography (SPECT)

Positron emission tomography (PET) and single photon emission computed tomography (SPECT) enable visualization of function and not anatomy of the body. Both techniques measure emissions from radioactive tracer which are injected into the bloodstream. These trace specific biochemical reactions or the distribution of a substance, e.g. the uptake of glucose. While both techniques detect photons, the process in PET imaging always produces pairs of photons and the detector only consider pairs as a valid signal. In SPECT imaging every single photon is counted and a lead collimator is needed to determine the origin of these. The collimator blocks most of the signal and SPECT is therefore less sensitive compared to PET. Only PET imaging can be used for quantification of the activity. The tracers used in SPECT last longer than those for PET which enables longer lasting effects to be measured. The spatial resolution is worse than other imaging modalities. Typical applications are localization of tumors and metastases and measurements of myocardial perfusion. PET is increasingly combined with CT and also MRI to produce images that show both anatomy and function.

3.2.2   Ultrasound features and applications

Which imaging modality is the most appropriate depends on the application. Both X-ray/CT and MRI have good signal to noise ratio. SPECT and PET measures physiological function and the choice between the two depends on which particular function is of interest. However, X-ray/CT, PET and SPECT are all associated with a non-negligible amount of radiation. Some patients feel claustrophobic during CT and MRI examinations. Also, all of the above mentioned modalities require the patient to be moved to the location of the machine and are all relatively expensive.

Ultrasound on the other hand is portable, low-cost, free of radiation and not associated with any discomfort for the patient. Further, ultrasound has a good spatial- and temporal resolution and displays images in real time. The drawbacks include limited depth penetration (especially in lung- and skeletal applications), relatively poor signal to noise ratio and need of experienced operators.

Ultrasound is extensively used in cardiovascular applications including examinations of the heart, aorta and carotid arteries. Echocardiography (cardiac applications) include e.g. quantification of size and shape, evaluation of cardiac function, detection of tumors and damaged tissue and blood flow measurements. Carotid arteries are typically scanned in patients suspected to have developed atherosclerotic plaques, in which case the plaque size and the degree of stenosis is measured. The latter by means of blood velocity measurements (blood velocity increases with increased stenosis). Ultrasound is also used to image a large number of other soft tissues such as liver, kidneys, breasts, thyroid gland, muscles and testes. Another application where ultrasound is extensively used is obstetrics. In many countries fetuses are routinely examined in order to estimate the date of birth. Obstetric ultrasound can also provide important information about the development of the fetus and the health of the mother throughout the pregnancy. Finally, ultrasound is useful as guidance during invasive procedures, e.g. biopsy and tumor removal, where ultrasound images are effectively used to guide surgical tools.

Regarding the assessment of vulnerable plaques, several such methods based on all types of imaging modalities have been presented during the last decade. Methods, based on ultrasound, CT and MRI all have their inherent advantages in characterizing vulnerable plaques.[11] There is currently no superior imaging modality for this task, however in a wider use ultrasound has the benefit of being safe, time-efficient, easily tolerable and relatively cheap. This modality is therefore one of the most promising when it comes to screening of high risk patients.

4. ARTERIAL CHARACTERIZATION USING ULTRASOUND

4.1 Motivation

Arterial characterization is a term commonly used when it comes to quantify properties of arteries, in our case mechanical and/or acoustic. Using ultrasound a parameter of interest is measured either visually in the ultrasound image, by motion tracking, by Doppler or by measuring properties (e.g. spectral) of the raw signal. Ultrasound imaging of arteries is an important tool both to detect and diagnose atherosclerosis and to study the progression of it. Arteries are routinely examined in clinics today and a vast majority of these examinations are made on the carotid artery, both because it is very accessible and because it is a site prone to develop atherosclerotic plaques. Using 2D ultrasound the artery can be visualized either longitudinally or transversely (see Fig. 7).

The examinations mainly involve measurement of maximum blood velocity assessed with Doppler. Together with the degree of stenosis (how much of the artery a plaque obstructs) the outcome decides whether the patient should undergo endarterectomy (surgery to remove plaque). However, such measurements are poor indicators of whether a patient needs surgery or not and there is no method in clinics today for early detection of emerging atherosclerosis. Therefore, there is a need for accurate and robust methods that could aid the clinicians both to detect early stages of atherosclerosis and to characterize plaque vulnerability. Ideally, a clinically applicable imaging modality should be time-efficient, non-invasive, low-cost, easily tolerable, give real-time results and with no use of radiation, contrast or manual post-processing. The techniques that embrace most of these demands are ultrasound-based. In the subchapters below several different methods that are developed for arterial characterization (of which most have not yet reached clinics) will be introduced.
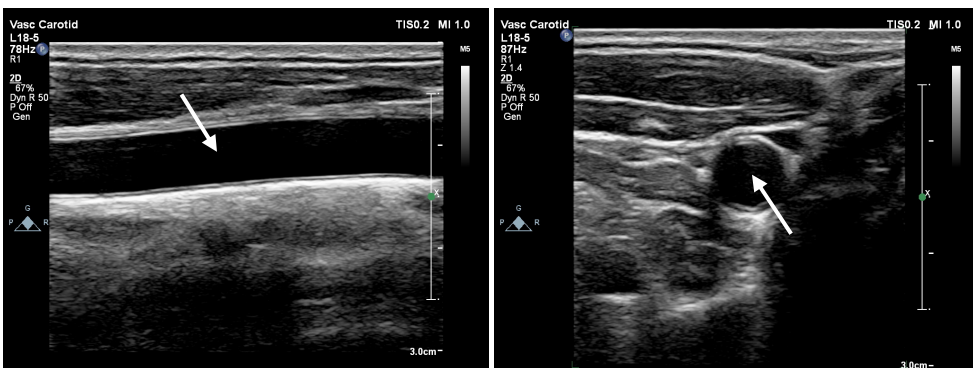

Figure 7. B-Mode images of a longitudinal (left) and transverse (right) cross-section of a human carotid artery. The arrows indicate the center of lumen (where the blood flows).

4.2   Diameter and intima-media thickness

An early indication of atherosclerosis is thickening of the arterial wall due to migration and proliferation of smooth muscles cells and accumulation of lipids (see chapter 2). Another early marker is stiffening (stenosis) which makes the wall less elastic. Therefore, measurements of wall thickness and elasticity may have significant clinical relevance as an early marker facilitating future assessment of cardiovascular events.[12]

Measurements of arterial wall thickness and diameter is usually performed in the longitudinal view (see Fig. 7). As can be seen the arterial wall appears with a double line pattern. The first (inner) line stems from the intima-media complex where the boundary between the intima and media cannot be resolved. The second (outer) line stems from the adventitia. Since the atheroma (accumulation of degenerative material) occurs in the intima layer, which cannot be visually resolved from the media, the atherosclerotic thickening of the arterial wall first appears as an increased distance between the first and second line in the ultrasound image. The thickness of the wall is called the intima-media thickness (IMT) and defined as the distance between these two lines. The diameter is defined as the distance between the intima-media complex of the near and far wall (see Fig. 8).

The elasticity can be assessed by measuring the dynamic behavior of the artery as it repeatedly distend (enlarge) radially as a response to the pulsatile blood flow. Stiffer arteries will show less distension than more elastic healthier arteries. The distension is defined as the difference in systolic and diastolic diameter (max and min diameter).
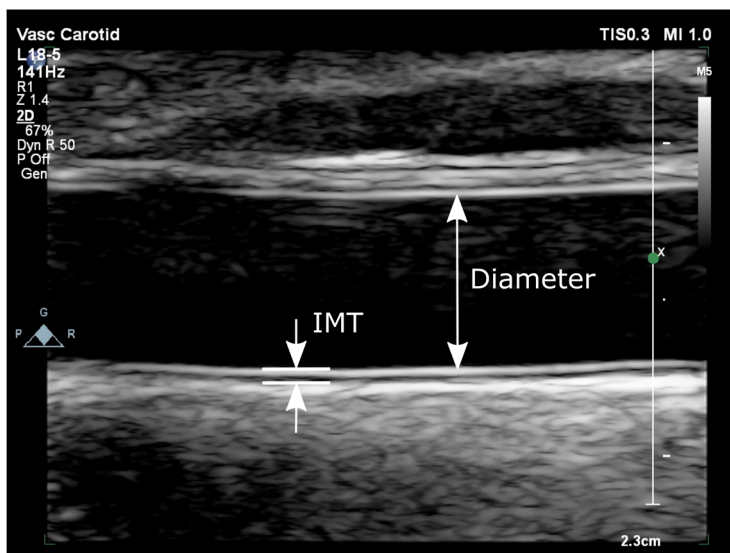
Figure 8. The diameter and intima-media thickness (IMT) of a carotid artery.

A direct physical measure of the elasticity is difficult to achieve since the true local pressure is unknown. Usually, the blood pressure is measured in the brachial artery using a cuff or by applanation tonometry. Several parameters that are associated with elasticity have been defined and used including strain, elastic modulus (Ep), stiffness index (β), distensibility coefficient (DC) and compliance coefficient (CC). See Table I for definitions.

Today measurements of carotid IMT and diameter are often performed manually by experienced observers. Such measurements are time-consuming, especially multi-frame analysis, and subjected to large variability between different observers, ultrasound scanners and datasets.[12] Hence, robust and accurate automatic methods for measuring arterial IMT and diameter are preferable if not required.

One of the first to measure arterial distension *in vivo* was Arndt et al.[13] who used a threshold technique to detect the arterial walls. They found that the distension was about ten times larger than previously reported. To avoid errors in threshold detection strategies due to change in echo amplitude, Hokanson et al.[14] used a phase locked technique to simultaneously measure both arterial walls. This method increased the resolution down to a few microns but failed if the wall moved more than half a wavelength between two transmissions. Another edge detection technique was presented by Cinthio et al.[15, 16] who used thresholds based on relative amplitudes to measure the arterial diameter and distension. High sub-pixel accuracy was achieved by solving the equation of a straight line between the two samples on either side of the threshold value.

Table I. Definition of different arterial stiffness parameters

Arterial stiffness parameter	Definition
Strain	$\dfrac{d_{systole} - d_{diastole}}{d_{diastole}}$
Elastic modulus	$Ep = \dfrac{P_{systole} - P_{diastole}}{Strain}$
Stiffness index	$\beta = \dfrac{ln(P_{systole}/P_{diastole})}{Strain}$
Distensibility coefficient	$DC = \dfrac{\Delta A/A}{P_{systole} - P_{diastole}}$
Compliance coefficient	$CC = \dfrac{\Delta A}{P_{systole} - P_{diastole}}$

d = diameter
P = pressure
A = cross-sectional area (inner)

Multi-gate Doppler is a technique were the artery is divided into several gates in which the velocities are measured individually and simultaneously. Depending on which filter is used either the tissue- or blood velocity is obtained. Thereby, both the velocity (and distension) of the arterial wall and the blood velocity distribution can be assessed simultaneously. Such methods were presented by Hoeks et al.[17] and Tortoli et al.[18]

An alternative method to derive arterial stiffness *in vivo* was derived by Khamdaeng et al.[19] They measured the stress-strain relationship using applanation tonometry together with 1D cross-correlation to assess pressure and wall displacement. The elastic modulus was estimated based on different models. It was shown that there is a change in slope of the stress-strain curve relating to the different contributions of elastin and collagen fibers in the systolic phase of the cardiac cycle. This was used to estimate the elasticity and mechanical interaction of the arterial wall components.

Pignoli et al.[20] were the first to use ultrasound images to measure wall thickness. They found that the thickness of the typical double-line pattern in B-Mode images corresponded to the combined thickness of the intima and media layers. This introduced a new technical research area focused on developing computer assisted measurements of IMT. Since then a large number of different methods have been proposed and they are based on several different segmentation techniques. Once the arterial layers (double-line pattern) are segmented both the IMT and the diameter can be derived. The following references are examples of such techniques used for measuring IMT.

Liang et al.[21] used dynamic programming with a multiscale approach to segment the different layers. Different local parameters, the echo intensity, the intensity gradient and the boundary geometrical constraints where combined and weighted. This yielded a cost function which could be optimized to estimate the position of an arterial layer. The method also allowed for human intervention in order to allow varying image qualities.

Golemati et al.[22] utilized the Hough transform to segment the carotid artery in both longitudinal and transverse sections. The Hough transform is commonly used to extract features in image analysis, usually lines or circles, where a complex global detection problem can be converted to a simple peak-detection. The images were first pre-processed with filtering and morphological closing followed by edge detection before applying the Hough transform. They showed that this technique can be used for accurate IMT measurements provided that the artery was well represented by circles (transverse images) or straight lines (longitudinal images).

Another approach is snake based segmentation, which utilize the distinct double-line pattern. The snake can be seen as a set of consecutive vertices with lines between them that are distributed across the arterial wall. An optimization procedure is then used to move the vertices to form a line that is the most probable to represent an arterial layer. Loizou et al.[23] presented such a method which, together with a speckle reduction filter and image normalization, was used to segment the arterial wall.

Although the variability of IMT measurements are lower for computerized methods compared to manual measurements the semi-automatic methods are still better than the completely automatic methods.[12, 24] No method seems to outperform the other methods in all aspects and further developments are needed.[25] However, reviews of the most commonly used methods indicate that those developed by Ilea et al.[26] and Faita et al.[27] are among the best for segmentation of the intima-media complex.[12, 24] Ilea et al.[26] used a model-based approach to automatically segment the arterial walls in the first frame. These were then tracked automatically in the remaining frames using an adaptive normalized correlation. Faita et al.[27] used a gradient-based approach to locate the transitions between different arterial layers. They introduced a first-order absolute moment operator as a robust edge detector which also improved robustness to noise.

A significant correlation between increased IMT and risk for cardiovascular events has been established in several studies.[28] However, so far the addition of IMT measurements to traditional cardiovascular risk factors does not seem to significantly improve the prediction of a cardiovascular event.[28]

4.3   Longitudinal movement

Besides the radial distention caused by the pulsatile blood flow many arteries also exhibits a longitudinal movement, i.e. a movement parallel to the blood flow (see Fig. 9). For a long time the longitudinal movement was considered to be negligibly small or even absent.[3] The first notation of the longitudinal movement was made by Lawton and Greene[29] who made observations of beads sutured to the surface of the abdominal aorta. The movement was very small and respiratory movements of the diaphragm was considered to be the driving force. Later studies[30-32] supported the results obtained by Lawton and Greene. However, Tozzi et al.[33] demonstrated a significant length reduction of the carotid artery in pigs where they measured the time delay between piezoelectric crystals sutured to the surface of the artery. This was a strong indicator that there was in fact a significant longitudinal movement present.

By using ultrasound images our group was the first to report and measure a distinct longitudinal movement of the intima-media complex.[34, 35] It was shown that this movement was in fact of the same magnitude as the radial movement (see Fig. 10) and that the movement was larger in the intima-media complex than in the adventitia giving rise to an intramural shear stress.[36] Further, the longitudinal movement demonstrates a bidirectional tri-phasic pattern with an initial antegrade (along the blood flow) movement followed by a retrograde movement and then a second antegrade movement before returning to its initial position (see Fig. 10). We have shown that adrenaline can pronouncedly influence the longitudinal movement and the resulting shear strain within the arterial wall.[37, 38] Further, we have shown that a profound longitudinal movement can take place independently of wall shear stress.[39] These studies have opened up a new field within cardiovascular research, revealing a previously unknown mechanism in the circulatory system.
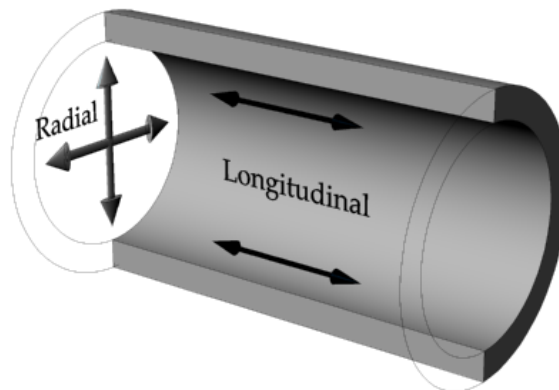

Figure 9. The directions of the radial and longitudinal movements of arteries.
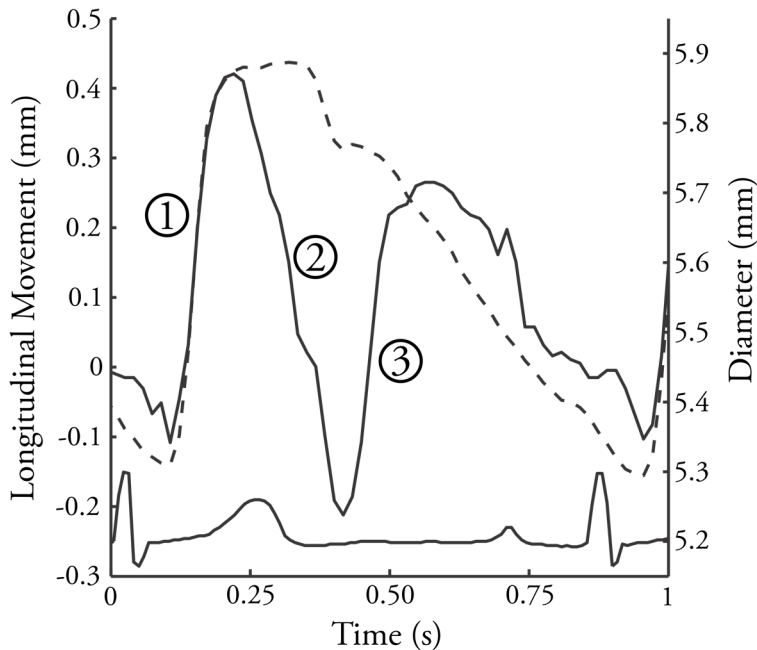
Figure 10. Typical pattern of the longitudinal movement (solid) and diameter (dashed) in the common carotid artery during a cardiac cycle. The longitudinal movement consists of an initial antegrade movement (1) followed by a retrograde movement (2) and then a second antegrade movement (3) before returning to its initial position. Bottom line shows the ECG.

A study by Warriner et al.[40] described a computational model supporting the existence of a longitudinal movement. Other groups have confirmed both the presence of the longitudinal movement and that there seems to be a connection to cardiovascular disease. Both radial and longitudinal movements were measured by Golemati et al.[41] using block matching. Also Zahnd et al. used block matching techniques to show that the longitudinal movement in older diabetic patients[42], in patients with periodontal disease[43] and in patients with high cardiovascular risk[44] (metabolic syndrome, or type 1 or 2 diabetes) was significantly smaller than in control groups. Svedlund et al.[45] used vector velocity imaging to measure the longitudinal movement in 441 patients with suspected coronary artery disease. Their result suggests that the longitudinal movement can be used to predict ischemia.

More studies are needed to establish the, so far unknown, mechanism behind the longitudinal movement. Expectantly, future studies will determine the physiological purpose of the longitudinal movement and the clinical value of measuring it.

4.4   Pulse wave velocity

Gradual stiffening of the arterial wall can be used as an early indicator of cardiovascular disease.[46-48] As mentioned previously the stiffening can be assessed by measuring the change in arterial diameter. However, the change in mechanical properties of the arterial wall also affects the velocity of an induced mechanical wave. A common way of assessing this is by measuring the pulse (pressure) wave velocity (PWV), i.e. the velocity of the pressure wave caused by a heartbeat. This velocity will increase as the arteries get stiffer and thus acts as an indirect measure of arterial stiffness. The relation is described by the Moens-Korteweg formula:

$$PWV = \sqrt{\frac{Eh}{2\rho R}},\tag{1}$$

where E is the wall elastic modulus, h is the wall thickness, ρ is the blood density and R is the arterial lumen radius.

Noninvasive ultrasound methods for PWV measurements can be categorized as either echo-tracking or Doppler-based. Echo-tracking methods measures the wall displacement using various motion tracking approaches. The Doppler-based methods measures blood velocity waveforms or utilize tissue Doppler to measure arterial distention. The most widely used principle is to measure the carotid-femoral PWV using the so called transit-time method. This means measuring the time delay between pulse arrival (foot-to-foot of the pressure or blood velocity waveforms) in the carotid and femoral arteries, yielding an overall average of the PWV in the aorta.[49-52] Unfortunately, this method is affected by the relatively large uncertainty in determining the pulse propagation length.[53, 54] The distance between the carotid and femoral arteries can only be measured at a coarse level and the arterial dimension is assumed to be constant. A more accurate approach would be to measure the PWV locally within a single ultrasound image where both the dimensions and distances are well known. Such methods are somewhat more difficult and requires high frame rate.

Benthin et al.[55] used a phase-locking technique to measure the local PWV on a phantom and in the carotid artery on young healthy individuals. Cross-correlation of analog RF data was used to measure the changes in arterial diameter at two different sites. They found artefacts due to reflected waves and modified the PWV estimation using only the foot of waveform to correct for the induced errors.

Brands et al.[56] estimated the local PWV in phantoms using temporal and longitudinal gradients of the measured change in diameter. Arterial distensibility was assessed using ECG triggering and signal processing of the RF data. This method was further

developed by Meinders et al.[57] including also real time B-Mode images which made it easier to maintain the artery within focus. An *in vivo* evaluation on the carotid artery in 23 patients yielded an average PWV of 5.5 m/s.

Another method to measure PWV involves the use of tissue Doppler imaging and was presented by Eriksson et al.[58] Using an *in vitro* set-up with an elastic vessel and a pulsatile pump it was shown that system parameters had a significant effect on the variance of the measured PWV, whereas the mean PWV was unaffected. They found that the most important parameter to obtain accurate estimates of PWV with low variance was high temporal resolution.

The PWV can also be determined from the ratio between the change in blood flow Q and the change in cross-sectional area A:

$$PWV = \frac{dQ}{dA}. \tag{2}$$

This so called area-flow (QA) method was first presented by Rabben et al.[59] in an evaluation on four dogs and 21 human subjects. There was a good agreement to the reference method, the Bramwell-Hill equation[60] which requires knowledge about blood pressure. However, they also concluded that improvements were needed to reduce the residual variance. In another study Williams et al.[61] compared the QA method (local) to the transit-time method (regional) using high frequency ultrasound in mice. They concluded that the methods correlated strongly with each other and that it is possible to measure PWV in mice with high frequency ultrasound.

Pernot et al.[62] showed a color-coded visualization of the PWV. Cross-correlation was used to measure the arterial distention and they used ECG triggering to achieve an extremely high frame rate of 8 kHz. The same method was used to measure the local PWV in normal and diseased abdominal aortas in mice[63-65], human subjects[66, 67] and also in the carotid artery in human subjects[68]. Figure 11 shows the propagation of the pulse wave in a normal aorta (mouse) using this method.[63]

Even though several promising methods for local PWV measurements have been presented during the last two decades, the carotid-femoral transit-time method is still the gold standard within clinical studies. Despite the limitations of coarse propagation distance measurements and assumptions of arterial dimensions, the transit-time method prevails. One reason might be that, although there is a strong correlation between local and regional measured PWV, the locally measured are generally lower than the regionally measured making comparisons to other (e.g. older) studies more difficult.[69]
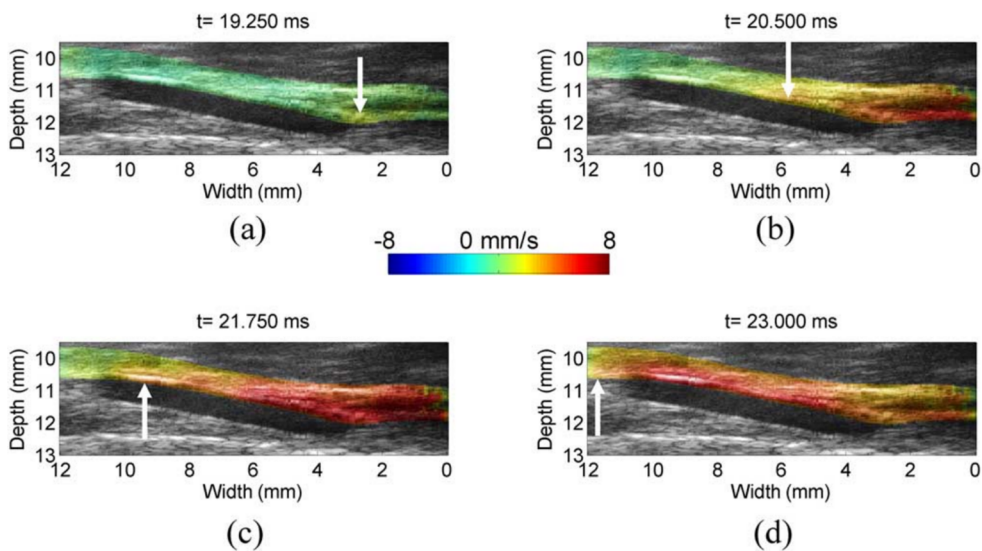
Figure 11. Color-coded (red up, blue down) tissue motion overlaid onto the B-Mode image every 1.25 ms in a normal mouse aorta. The titles state time after the R-wave of the ECG. White arrows indicate the propagation of the pulse wave from the proximal to the distal site (a)–(d). Luo et al.[63] © 2009 IEEE.

4.5   Plaque characterization

If the atherosclerosis continue unabated it will eventually result in the formation of one or several plaques. As described in chapter 2 an atherosclerotic plaque can be categorized as either stable or vulnerable. Vulnerable plaques are prone to rupture causing sudden events such as heart attack or stroke. The vulnerability of the plaque is mainly determined by its composition. A vulnerable plaque is characterized by a core of necrotic debris and lipids, an accumulation of inflammatory cells and a reduced content of fibrous tissue and smooth muscle cells.[70] A stable plaque mainly consists of fibrous tissue and smooth muscle cells.

In this chapter different ultrasound methods derived to characterize atherosclerotic plaques (and to some extent tissue in general) are presented. Plaque characteristics can be defined and measured in different ways. When it comes to ultrasound the methods could preferably be divided into those based on motion tracking, *elastography* and to those based on *single frame analysis*.

4.5.1 Elastography

The purpose of elastography is to measure how soft (or stiff) a region of tissue is. Different tissues have different mechanical properties and will respond differently to an imposed pressure. Soft tissue will compress more than stiff tissue if subjected to the same force. Elastography methods aim to measure the deformation, or strain, of a compressed tissue and thereby determine what kind of tissue it is. To measure this one requires at least two ultrasound acquisitions where there has been some deformation of the tissue in between. The position of a region of interest (ROI) is measured in both acquisitions and the difference (motion) between them is determined. Using two different ROI the relative deformation (change in distance between ROI) can be derived. The strain is then calculated as the relative deformation divided by the distance between ROI. Elastography is hence methodologically equal to motion tracking, which is a broader term.

The concept of ultrasound elastography was first introduced by Ophir et al.[71] However, Bonnefous et al.[72] were the first to attempt non-invasive elastography to assess atherosclerosis. They placed samples from excised human arteries in a pump system submerged in a temperature regulated bath. Blood and anti-coagulation drugs were circulated in a controlled pulsatile manner, mimicking normal blood flow. The radial strain was measured using a one-dimensional cross-correlation technique similar to that used in Doppler and compared to histology. They found a high correlation between actual lesion stiffness and radial strain measured with ultrasound.

Kanai and co-workers have developed a phase-tracking method[73, 74] which accurately estimates sub-sample motion based on time domain phase correlation of the RF data. If the local signal is assumed to be identical between two frames the difference in phase will correspond to the motion between those frames. Difficulty arises in the fact that the central frequency, affected by e. g. attenuation, needs to be known. A method to reduce the influence of the variance the central frequency was proposed.[75] This phase-tracking method was used to derive the elastic modulus of different tissue in atherosclerotic plaques.[76] By comparing to pathological findings, imaged tissue could be statistically categorized as lipid, mix or other. The same method was applied in 242 individuals with type 2 diabetes and shown to correlate with several risk factors for atherosclerosis.[77] The method also correlates to visceral fat area an independent variable affecting arterial elasticity.[78]

Using a 2D multi-level cross-correlation method Shi et al.[79] calculated the axial strain distribution within atherosclerotic plaques in the carotid artery *in vivo*. The lateral shift of the plaque, i.e. the longitudinal movement relative the arterial wall, was also measured. The maximum accumulated axial strain and the maximum relative lateral

shift could differentiate between non-calcified and calcified plaques as determined by visual interpretation of the B-Mode images. Maurice and co-workers derived an elastography method based on a Lagrangian speckle model estimator.[80, 81] This method reproducibly measured strain in the carotid artery in 16 individuals without previous history of atherosclerosis.[82]

Larsson et al.[83] performed a phantom study were a speckle tracking algorithm that measured radial, longitudinal and circumferential strains in the carotid artery was validated against sonomicrometry. Using both clinical- and high-frequency ultrasound images they showed that for circumferential strain measurements high-frequency ultrasound was favorable. Preliminary *in vivo* results using the same method show that echolucent plaques demonstrated higher strain than echogenic plaques.[84]

Intravascular ultrasound (IVUS) is commonly used to assess coronary plaques and because of the short distance between transducer and plaque, high transmission frequencies of typically 30-40MHz can be used. Schaar et al.[85] used IVUS to assess plaque vulnerability *in vitro*. Twenty four excised human coronary arteries were mounted and pressurized in a water column system containing physiological saline solution. A first IVUS frame was collected at an intravascular pressure of 80 mmHg and after 10 seconds another frame was collected at 100 mmHg. The resulting incremental strain in the tissue was measured using a method based on cross-correlation.[86] In the 24 arteries 26 vulnerable plaques and 28 nonvulnerable plaques were found. The criteria for vulnerable plaque, determined by histology, was a thin cap (<250 μm), moderate to heavy macrophage infiltration and at least 40% atheroma. In the elastography measurements a vulnerable plaque was defined as a plaque with a high strain region at the surface with adjacent low strain regions. The sensitivity and specificity to detect vulnerable plaques were 88 % and 89 %, respectively. The same method was also used in the first *in vivo* validation of IVUS elastography in a Yucatan pig study, demonstrating increased strains in fatty plaques.[87]

Recently Hansen et al.[88] performed a study combining compounding with ultrafast plane wave imaging (frame rate was 2000 Hz) for vascular strain measurements. Both simulation and phantom experiments were conducted. In the simulation a finite element model was used to construct a 3D model of a carotid artery with a vulnerable plaque and Field II[89, 90] was used for ultrasound simulation. A two layered phantom was also constructed with a soft inner layer and a stiffer outer layer. The plane wave compounding method outperformed traditional focused strain imaging and reduced the root mean squared error by 66% and 50% for radial and circumferential strain respectively.

Another increasingly used elastography method is shear wave imaging. Shear waves are waves that propagate perpendicular to the ultrasound field. Such waves can be induced using the acoustic force produced by focused ultrasound. Shear wave travels much slower and the velocity is directly related to tissue stiffness. Therefore, by measuring the propagation speed of the induced shear waves (using e.g. plane wave imaging), a quantitative tissue specific parameter can be determined. The use of shear wave imaging on the carotid wall, including atherosclerotic plaques, have been shown feasible.[91-93] Figure 12 shows an example of shear wave imaging of plaque in the carotid artery.[93]

Great progress have been made in elastography during the last decade, especially in shear wave imaging. However, more studies are needed. A review by Sarvazyan et al.[94] states that although plaque characterization using elastography shows promise, significant technical hurdles needs to be faced before clinical use becomes practical. Also, further studies on larger patient populations are needed to establish the clinical use.[95]
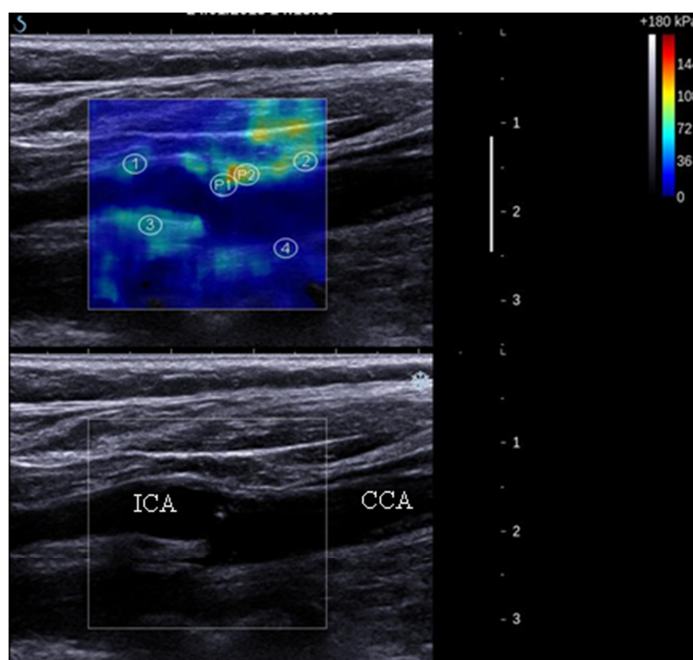

Figure 12. Shear wave imaging (above) of a carotid plaque with different proposed region of interests 1-4. Below is the corresponding B-Mode image of the common carotid artery (CCA) and internal carotid artery (ICA). © Ramnarine et al.[93] 2014.

4.5.2 Single frame analysis

The term single frame (tissue-) analysis is used to distinguish methods from those based on motion tracking e.g. elastography which by nature requires multiple frames to obtain a result. Methods based on single frame analysis are methods which, in one way or another, characterize tissue based on features of the ultrasound data. Such methods could obtain results using a single frame, although it is common to use the average of several to improve accuracy.

B-Mode statistics

One category of methods are those that use different, often statistical, features of the ultrasound B-Mode images. The idea is to find mathematical tools to derive statistical differences in B-Mode images corresponding to different types of tissue. Such features are based solely on the amplitude information and are thus subjected to potential inaccuracies followed by the manipulation of operator dependent settings and differences in pre-image signal processing between scanners. For instance the pre-defined gain and time-gain compensation (not necessarily linear) may differ between scanners and may also partly be adjusted be the operator. Many such amplitude based methods have been derived and a few examples are mentioned below.

Perhaps the most recognized amplitude-based method for use on arteries is the so called gray-scale-median (GSM). This parameter measures the median amplitude value within a ROI (usually a plaque). El-Barghouty et al.[96] compared GSM on carotid plaques to the corresponding histology in 52 patients undergoing carotid endarterectomy. Plaques with a high amount of lipids and hemorrhage had low GSM (r=-0.351, p<0.05) and those with a high amount of fibrous content had high GSM (r=0.411, p<0.001).

Later Wilhjem et al.[97] evaluated 16 first order and seven second order texture statistics as well as GSM in carotid plaques in 52 patients scheduled for endarterectomy. First order textural statistics included e.g. maximal and minimal gray level, skewness, kurtosis, energy, entropy and (histogram-) percentiles. Second order textural statistics included e.g. correlation, diagonal moment and contrast. The plaques were scanned in the lateral, anterior and cross-sectional planes and the data divided into a training and a test set. Results were compared to histology where the GSM correlated to the relative volume of soft materials defined as lipids, hemorrhage, and thrombus (r=-0.42, p=0.002). The best match was the second order parameter related to contrast (r=0.5). However, they stated that although a few features reach significant correlation the

training and test errors were much too high for the method to be used in prediction of relative volumetric content in individual plaques.

Also coronary arteries have been studied using IVUS. Vince et al.[98] compared five different texture analysis methods in their ability to distinguish plaques with different components. Different regions were chosen from 27 coronary plaques classified as either calcified, fibrous or with necrotic core. Haralick's method[99], which is a second order parameter yielded the most accurate results. After optimization the error in separating plaque regions in different classes was 6.67%.

Tsiaparas et al.[100] studied 11 symptomatic and nine asymptomatic carotid plaques to compare different methods (e.g. the discrete wavelet transform, wavelet packets and the Gabor transform) based on spatial frequencies in their ability to discriminate between symptomatic and asymptomatic cases. Of the evaluated methods the results suggests that wavelet packets used with coiflets together with support vector machine learning is the most appropriate for analyzing atherosclerotic plaques. Although a limited number of plaques were evaluated the overall accuracy was 82.5%.

In another study Kakkos et al.[101] aimed to identify textural features of carotid plaques which are independently associated with amaurosis fugax (AmF), transient ischemic attack (TIA) and stroke. They included 43 asymptomatic patients (51 hemispheres) and 137 patients (137 hemispheres) with AmF (n = 30), TIA (n = 52) and stroke (n = 55). A total of 51 histogram and texture features including GSM was evaluated. Principal component analysis yielded independent features for each of the above mentioned ipsilateral hemispheric symptoms. The result showed that the major determinant for AmF and stroke was echolucency while for TIA it was plaque homogeneity. They also found that symptomatic plaques were more homogeneous than asymptomatic.

Attenuation measurements

As an ultrasound pulse propagates though a medium its amplitude is attenuated and high frequencies are attenuated more than low frequencies. This means that the amplitude of a pulse frequency spectrum decreases more rapidly for higher frequencies pushing the main energy towards the lower frequencies. In many tissue characterization methods this is considered to be a problem that needs to be compensated. However, this physical effect can be used in itself as a measure of a tissue specific property since different tissues attenuates the ultrasound by different amounts. In either case ultrasound attenuation is often something that need to be dealt with.

The most straightforward technique to measure attenuation is though transmission, i.e. when the sound has propagated through and left the sample. This is rarely applicable on living tissue. The concept of measuring attenuation in reflected and scattered ultrasound is more complicated involving instrument related factors and the effect of the scattering tissue. This is often best performed using the ultrasound RF data and commonly the attenuation coefficient is assumed to be linearly dependent on frequency.

The study of Kuc and Schwartz[102] counts as pioneering in measuring attenuation in reflected ultrasound comparing the power spectrum of the RF data for different depths in samples of liver *in vitro*. Assuming a Gaussian shaped pulse, Fink et al.[103] used short-time Fourier analysis and tracked the spectral centroid to derive attenuation coefficients on phantoms. At the same time Flax et al.[104] derived a time domain method where the attenuation was measured by counting the zero-crossings in the RF data.

Atherosclerosis has been shown to alter the attenuation coefficient in tissue. Picano et al.[105] studied 400 sections of fresh human aorta taken from autopsy. Using histology these were categorized as either normal aortic wall, fibrous plaque, fibrofatty plaque or calcified plaque (100 sections each). A specular reflector was placed behind the sample and the attenuation was then determined based on the echoes produced by this reflector both in the presence and absence of the sample. The result showed increasing attenuation starting from normal tissue to fibrous, fibrofatty and calcified. Shi et al.[106] derived a power difference method for accurate and unbiased estimations of the attenuation in small *ex vivo* samples of carotid plaque encased in gelatin phantoms. The method gave significantly lower values than traditional methods.

In an interlaboratory study and using three different clinical scanners Nam et al.[107] measured the attenuation (and backscatter) coefficient of layered phantoms mimicking the heterogeneous tissue often overlaying the tissue of interest in *in vivo* applications. The aim was to assess the accuracy of backscatter and attenuation measurements in such inhomogeneous tissue propagation paths. The constructed tissue-mimicking phantoms had three layers and, as a reference, the attenuation coefficient was measured using a narrow-band substitution technique. Each laboratory then measured the attenuation with the clinical scanners according to the reference phantom method[108, 109] but independently chose specific analysis parameters. The results were in excellent agreement with the narrowband substitution technique demonstrating that attenuation can be accurately estimated in layered media using clinical scanners.

In another study Labyed and Bigelow[110] compared the performance of three commonly used methods, the spectral log difference, the spectral difference and the hybrid method. Specifically the performance was evaluated when the ROI was heterogeneous

26

in terms of scatter number density and scatter size. The spectral difference method had highest accuracy when the ROI was homogeneous, however completely failed when the scatter number density varied. The spectral log difference and the hybrid method gave good results in both cases. However, when the scatter size varied within the ROI all methods failed.

Spectral analysis

Methods based on spectral analysis by definition use features of the frequency spectrum of the ultrasound RF data. As mentioned in the previous section one such feature could be the change in frequency with depth. But there are also other aspects of the backscattered data which are tissue specific and affects the frequency content. The backscattered energy will depend on scatter properties such as size and shape relative the wavelength and propagation direction of sound[111] and as a result the spectrum of a backscattered pulse will be dependent on scatter characteristics. The frequency content depends on scatter size, shape and elastic properties while the magnitude depends on size, scatter density and scatter strength. A theoretical framework for tissue characterization using spectral analysis was described by Lizzi et al.[112, 113]

Later Insana et al.[114] derived a theoretical model describing the effect of the average particle size and the acoustic concentration (product of the number density and the scattering strength) on the frequency spectra. The power spectrum of the RF data from a test material, consisting of either glass or polystrene microspheres, was normalized to a reference spectrum obtained from a Lucite plate placed in water. Scatter size estimation was performed by comparing the result to theoretical form factors obtained using the theory of Faran[115]. They found that the optimal range for estimating scatter size was $0.5 < ka < 1.2$ were k is the wavenumber and a is the scatter radius. Specifically they were the first to introduce the concept of acoustic form factors which relate the normalized spectrum to the correlation function of the medium. The form factors could be used to match a normalized spectrum to the response of a specific scatter size. In another paper Insana and Hall[116] showed that it is possible to image scatter size and strength using also commercially available imaging systems.

The methodological procedure mentioned above where the backscattered spectra is normalized to a reference spectra is the most commonly used to assess scatter characteristics. The reason for a spectral normalization is to remove the frequency dependence inherent to the instrumentation. The reference method (to obtain a reference spectra) was first presented by Madsen et al.[108] and further developed by Yao et al.[109]

Spectral analysis for tissue characterization has been used in a large number of studies to assess e.g. liver[113], ocular tumors[117], mammary tumors in rat[118] and breast cancer in humans[119]. The most interesting studies from the aspect of this dissertation are the studies on atherosclerotic plaques. Noritomi et al.[120] measured the slope, intercept and total power on the spectra from 299 ROI obtained from 19 carotid plaques *in vitro*. Plaques were assessed with histology and classified as fibrous, lipid or thrombus. The difference between fibrous plaques and the other two tissues was significant ($p<0.01$) for all parameters used alone. Lipid and thrombus plaques were significantly differed by intercept ($p<0.01$) and total power ($p<0.02$) but not for slope.

Bridal et al.[121] measured the integrated backscatter, frequency dependence of backscatter, integrated attenuation and slope of attenuation *in vitro* in 15 highly stenotic carotid plaques. Using histology 59 independent plaque sections were grouped as calcified, lipid, intraplaque hemorrhage, mixed or thrombus. All parameters except the slope of the attenuation was able to discriminate at least one of the groups from the others. However, no parameter was able to discriminate between all groups. If only considering the calcified, lipid and intraplaque hemorrhage sections a separation with classification boundaries could be derived. Correct classification was obtained for 100% of calcified, 75% of intraplaque hemorrhage and 71% of lipid plaques. Further, Waters et al.[122] measured the integrated backscatter, midband, slope and intercept of a straight-line fit to the backscatter transfer function. These parameters were compared to histology on 82 ROI from 17 carotid plaques *in vitro*. They concluded that integrated backscatter and midband showed good agreement in morphology with the histological images.

Shi et al.[123] showed preliminary results from *in vivo* measurements of attenuation and equivalent scatter size in 10 carotid plaques. Plaques were classified as either calcified or soft by an experienced radiologist based on B-Mode and color Doppler images. They found that calcified regions differed from softer regions in both scatter size (120-180 μm vs 280-470 μm using the theory of Faran) and attenuation (1.4-2.5 dB/cm/MHz vs 0.3-1.3 dB/cm/MHz). Later Yamada et al.[124] showed that integrated backscatter was clinically useful for monitoring atherosclerotic lesions. Forty patients with moderate carotid artery stenosis were randomly assigned to a diet group or a statin group. The latter was given lipid-lowering atorstatin. After a six months follow up the relative lipid volume, measured with integrated backscatter, was significantly decreased in the statin group whereas the diet group showed no significant difference.

Spectrum analysis has also been performed on IVUS images. Nair et al.[125, 126] used statistical classification trees where a combination of different spectral parameters (e.g. slope, midband and *y*-intercept) was used to classify plaque regions as calcium,

calcified-necrosis, fibrous or fibro-lipid. The predictive accuracy of this method, called virtual histology, was 79.7% (fibrous), 81.2% (fibro-lipid), 92.8% (calcium) and 85.5% (calcified-necrosis). Another method based on shadow detection, feature extraction and histogram analysis was presented by Taki et al.[127] This method, called imaged based histology, improved the longitudinal resolution compared to virtual histology.

Also integrated backscatter has been used on IVUS images. Kawasaki et al.[128] studied the integrated backscatter on 18 coronary plaque segments from nine patients. Sections were categorized using histology as calcified, mixed lesion, fibrous, thrombus, lipid core, intimal hyperplasia or media. There were significant differences between all categories but the values for lipid core, intimal hyperplasia and media were however quite similar. In the same study the integrated backscatter was compared to angioscopy where the color of the plaque can be visualized. It was found that the color seen in angioscopy mainly reflects the fibrous cap thickness and not the size of the lipid core. Since the integrated backscatter could detect both the lipid core and the fibrous cap it was considered more precise than angioscopy to characterize coronary plaques.

Seabra et al.[129] developed an IVUS method based on a mixture of Rayleigh distributions which were used to describe fibrotic, lipid and calcified plaques. As shown in an IVUS study by Katouzian et al.[130] there are however difficulties in tissue characterization due to *in vitro*, *in vivo*, inter- and intraframe variations of tissue spectra. This study also presented a texture-based plaque characterization method used to derive prognosis histology images which together with examples from other algorithms are shown in Fig. 13.
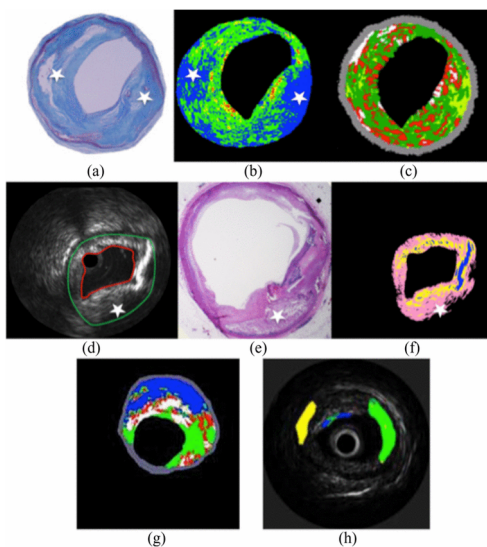
Figure 13. Examples of color-coded tissue maps from different plaque characterization algorithms based on intravascular ultrasound (IVUS). (a) Histology image and corresponding color-coded tissue maps from (b) the integrated backscatter algorithm[128] and (c) the virtual histology algorithm[126]. (d) B-Mode image with (e) corresponding histology and (f) color-coded tissue map from the prognosis histology algorithm[130]. (g) Color-coded tissue maps from the image based histology algorithm[127] and (h) the Rayleigh mixture model algorithm[129]. Katouzian et al.[130] © 2012 IEEE.

All reported methods used for scatter characterization are based on spectral analysis and are therefore subjected to a trade-off in time-frequency resolution. This has been shown both theoretically and practically by Gerig et al.[131] who concluded that the variance of scatter size estimates increase with decreased gate length.

Time domain phase analysis

The main subject in this dissertation is the use of time domain phase data for plaque/tissue characterization. Time domain parameters (except amplitude-based) are rarely used in single frame analysis (as mentioned previously zero-crossing techniques for measuring attenuation have been proposed[104]). However, we hypothesize that the use of time domain phase data could be beneficial in some aspects compared to spectral analysis. This section will introduce the instantaneous frequency and an autocorrelation approach to measure the center frequency in the time domain.

The gradient of the phase in the time domain, usually referred to as the instantaneous frequency[132] (IF) is commonly defined as

$$\varphi = \frac{\delta\omega}{\delta t},\tag{3}$$

where ω denotes angular frequency and t denotes time. The IF of a real signal can be derived using the orthogonal signal obtained by the Hilbert transform. If the data is sampled the discrete Hilbert transform is usually calculated by means of the discrete Fourier transform (DFT) given by

$$X(k) = \sum_{n=0}^{N-1} x(n) \cdot e^{-\frac{i2kn}{N}} \quad k \in \mathbb{Z},\tag{4}$$

where $X(k)$ are complex numbers describing the amplitude and phase for the frequency k/N cycles per sample of the real signal x. In order for the signal to be phase shifted by 90 degrees the last half of the complex values (corresponding to the negative frequencies) are first set to zero. The complex values are then transformed to a real signal using the inverse DFT given by

$$\hat{x}(n) = \frac{1}{N} \sum_{k=0}^{N-1} X(k) \cdot e^{\frac{i2kn}{N}} \quad n \in \mathbb{Z} \quad X_{|k>\frac{N}{2}} = 0.\tag{5}$$

The discrete IF is then calculated as

$$IF(n) = \frac{f_s}{2\pi}\left(arctan\left(\frac{\hat{x}(n)}{x(n)}\right) - arctan\left(\frac{\hat{x}(n-1)}{x(n-1)}\right)\right), \quad (6)$$

where f_s is the sampling frequency. The accuracy of the IF depends on the accuracy of $X(k)$ (eqs. 4-5) which in turn depends on the sampling rate and the gate length of the DFT. An important difference between the IF and the frequencies calculated with DFT is that for the IF the spatial resolution does not equal the gate length. In fact maximizing the gate length to an entire RF-line will maximize the *sample-wise* accuracy of the IF.

The mean frequency in the spectrum of a signal is equal to the mean IF.[132] However, precise interpretation of *sample-wise* IF from multicomponent signals (e.g. pulsed ultrasound) is difficult, if not meaningless.[132] However, if the effect of phase-shifts[132, 133] is considered to be small, we assume that the mean IF over a few wavelengths can be used to estimate the mean spectral frequency (see Fig. 14).
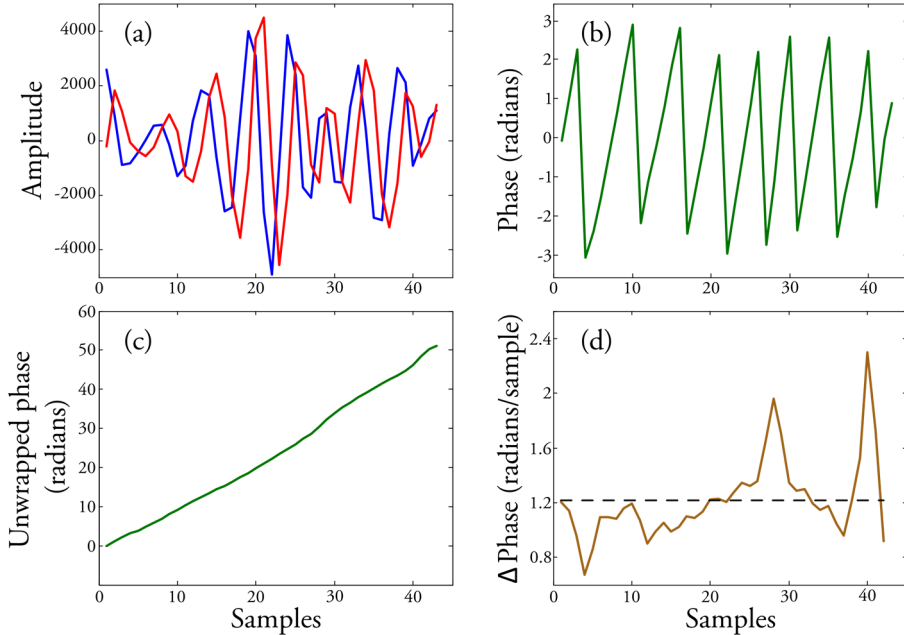
Figure 14. A method to estimate the center frequency using the time domain phase. a) The RF data (blue) and its orthogonal signal (red) obtained using the Hilbert transform. b) The phase of the RF data calculated as the arcus tangent of the signals in a). c) The same as in b) but unwrapped to remove phase jumps. d) The differentiated unwrapped phase (brown) and its mean value (dashed). If the data in d) is multiplied with the sampling rate (50 MHz) and then divided by 2π it gives the instantaneous frequency. Using a mean value of 1.219 radians/sample this yields an estimated mean center frequency of 9.706 MHz.

The mean IF is thus a center frequency estimator given by

$$\overline{IF} = \frac{f_s}{2\pi ab} \sum_{k_1}^{k_a} \sum_{l_1}^{l_b} arctan\left(\frac{\hat{x}(k,l)}{x(k,l)}\right) - arctan\left(\frac{\hat{x}(k-1,l)}{x(k-1,l)}\right), \quad (7)$$

where k_x and l_y denotes samples in a region bound within a by b samples.

If the entire RF-line is used in the Hilbert transform (eqs. 4-5) the accuracy of the mean IF will be substantially improved without affecting the spatial resolution. Assuming that a larger number of regions are to be evaluated this will also be more computationally efficient, compared to using DFT within each region, since the Hilbert transform is only calculated once for leach RF-line. The spatial resolution equals the size of the averaged region which needs to be large enough to cover effects of noise, phase-shifts and natural variations in IF due to the summation of multiple broadband pulses.

Another method to derive the center frequency is the complex autocorrelation method used in color Doppler ultrasound by Kasai et al.[134]:

$$R(n) = \frac{1}{N} \sum_{i=n-N/2}^{n+N/2} C(i)C^*(i-1), \quad (8)$$

where C^* denotes the complex conjugate. Note that in Doppler applications i represents the same sample from *different* transmitted pulses whereas in our case it represents different samples from the *same* transmitted pulse. The phase difference and thus the center frequency is obtained as the argument of $R(n)$:

$$f_{center}(n) = \frac{f_s}{2\pi} arctan\left(\frac{Im(R(n))}{Re(R(n))}\right). \quad (9)$$

Both equations 7 and 9 assess the center frequency by the calculating an average phase difference between time domain samples. As shown by Sirmans and Bumgarner[135] the autocorrelation method is unbiased for symmetrical spectra and superior in terms of accuracy and noise immunity compared to e.g. DFT. It was also shown that the bias caused by non-symmetrical spectra is rather small.

Measurements of center frequency in the time domain therefore seems to be more accurate than in the frequency domain (spectrum analysis). However, in contrast to spectral analysis, the methods described above only yields one frequency, the center frequency.

5. INTRODUCTION TO INCLUDED PAPERS

My work during the PhD studies have spanned several different areas of arterial characterization. In the included papers five different methods are presented. Two of these methods, presented in papers I-III are based on the time domain phase of the ultrasound data. The time domain phase comes with advantages in resolution and also naturally incorporates sub-pixel estimations in motion tracking (paper III). Generally this approach is also more computationally efficient compared to spectral analysis (papers I and II) or cross-correlation (paper III). Although we have not performed quantitative measurements of PWV, the method presented in paper III is suitable for measurements of both radial and longitudinal PWV, which have been visualized. Paper IV-VII presents methods for measurements of IMT, diameter and longitudinal movement.

Next pages outline a short introduction on each of the included papers. They are presented in reversed chronological order of development.

5.1   Paper I – overview

The frequency content of the reflected ultrasound pulses depends both on the instrumentation settings and on the characteristics of the scatters in the medium being examined. Specifically, when the scatter sizes are in the range of the wavelength of the ultrasound, the size is the dominating scatter property affecting the frequency spectrum of the backscattered data. In this paper we aim to derive a method for measuring scatter size using only the center frequency. The rationale for this, compared to methods based on spectral analysis, is that the center frequency can be determined in the time domain. Thereby, the measured shift in center frequency is not limited by the typical time vs frequency trade-off coupled with spectral analysis.

To evaluate the derived method five agar phantoms were made with well-defined sizes of glass beads. The phantoms were placed in water and scanned with two different transducers and six different center frequencies. The result (Figs. I-A and I-B) showed that there is a clear correlation between the normalized center frequency and scatter size and that it is feasible to measure scatter size using only the center frequency.
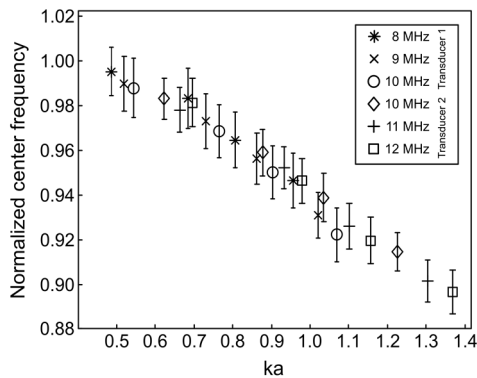
Figure I-A. The normalized center frequency as a function of the product ka (where k is the wavenumber and a is the scatter radius).
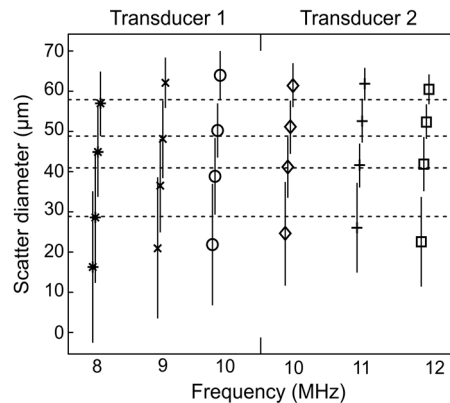
Figure I-B. Estimated scatter diameter (mean and standard deviation) for different transducer center frequencies. The dashed lines indicate the actual diameters in the four phantoms evaluated.

5.2   Paper II – overview

The vulnerable plaque is a plaque prone to rupture and is characterized by thin fibrous cap, relatively large amount of lipids, macrophages and hemorrhage. On the contrary, a stable plaque is considered to be composed of fibrous tissue and smooth muscle cells. The identification of vulnerable plaques remains a great challenge in clinics today. The center frequency of the reflected ultrasound pulses is related to scatter properties of the tissue in the plaque (see also paper I). The aim of this paper was to evaluate whether the time domain derived center frequency can be used to determine carotid plaque vulnerability.

The method was evaluated both *ex vivo* and *in vivo* on a total of 206 different fragments of carotid plaques. In both cases the measured center frequency shift (CFS) was compared to histology were the percentage of lipids, macrophages, hemorrhage, collagen and smooth muscle cells were measured. To assess the overall vulnerability of the plaque a vulnerability index was used with unstable components (lipids, macrophages and hemorrhage) in the numerator and stable components (collagen and smooth muscle cells) in the denominator. Figure II shows the method used on plaques with unstable (top and middle) and stable (bottom) phenotypes. The CFS correlated strongly with the vulnerability index and the accuracy to detect plaques with high vulnerability index was 78%, with sensitivity 77% and specificity 78%. This could improve preventive strategies, risk stratification and monitoring of interventions.
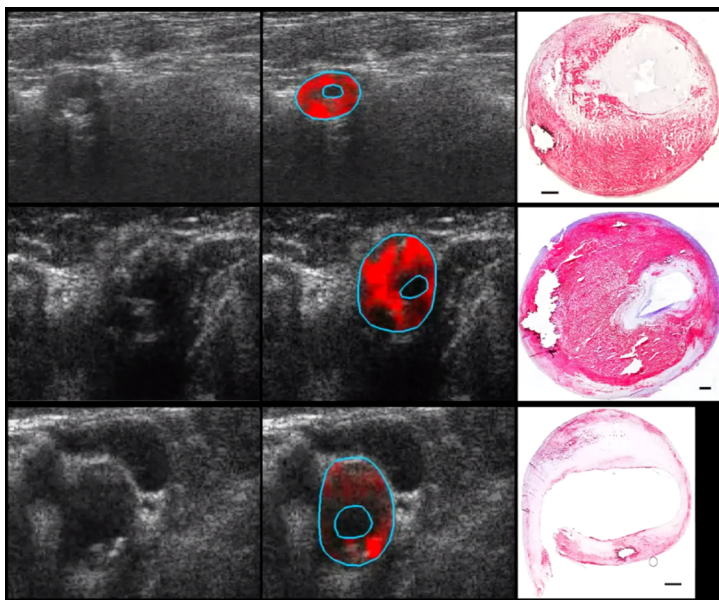

Figure II. Plaques with unstable (top and middle) and stable (bottom) phenotypes assessed with B-Mode (left), center frequency shifts (CFS) (middle) and histology (right) for lipids (more red equals more lipids).

5.3   Paper III – overview

Motion tracking is increasingly common in ultrasound tissue characterization methods. The key idea is to measure differences in regional compression due to an applied force – either external caused by the operator or internal caused by e.g. the pulsatile blood flow. The vast majority of motion tracking algorithms used in ultrasound applications are based on cross-correlation. Two drawbacks with such a method is that 1) they quickly become time-consuming when an increasing number of ROIs are used and 2) they require additional calculations to acquire sub-pixel resolution. The aim of this paper was to develop a new motion tracking algorithm that simultaneously solved both issues mentioned above.

The developed method transforms the amplitude information (B-Mode) to spatial phase information. This is performed in the time domain meaning that each pixel has its own phase (complex representation of amplitude information) and the phase does not relate to different frequency components as in the frequency domain. Because of the unique feature that speckle causes a rather uniform spatial frequency in the ultrasound image, the phase information could be locally approximated with a straight line. The motion for each pixel can then be calculated using the equation of a straight line, knowing the difference in phase for each pixel between two frames and the gradient of the local phases.

The method was evaluated on phantoms and on the longitudinal movement (see Fig. III) of the arterial wall.
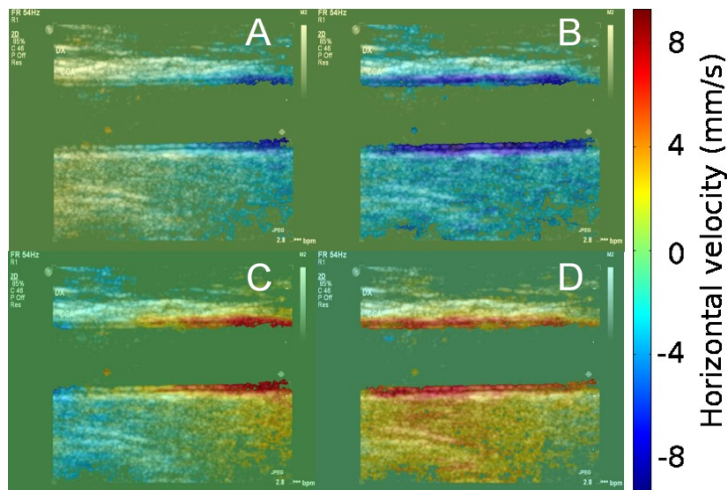

Figure III. Four consecutive frames (A-D) where two phases of the longitudinal movement can be visualized.

5.4   Papers IV and V – overview

The diameter and intima-media thickness (IMT) of the arterial wall can be used to measure early signs of atherosclerosis. Although today there exist several computerized methods, manual measurements are still dominating. One reason may be a lack of robustness in the automatic methods. Most methods are likely developed using images from a single ultrasound scanner and/or a single type of artery, e.g. the carotid artery. However, the appearance of the arterial wall strongly depends on the scanner used, which artery is imaged and the age, health and type (human/animal) of subject. The overall aim of these papers was to develop a robust method for diameter and IMT measurements working on different scanners, arteries and on different types of patients.

The method uses a combination of peak and threshold detection to segment the different layers of the arterial wall (Fig. IV). The specific threshold values were based on several hundred different images from different scanners, arteries and subjects. Overall the result was satisfactory since the method works, without any modifications, equally well on a variety of cases including diameters ranging from 0.65-13.8 mm and IMT ranging from 72-1620 μm (unpublished data).

In paper IV the method is evaluated on the aorta of premature rabbit pups. This was the first time that diameter and intima-media thickness was measured simultaneously and automatically in a small animal model. The inter-observer variability was decreased compared to manual measurements and the results showed that the method could be a useful tool for arterial characterization in small animals. In paper V the method was evaluated on the carotid artery in patients with different age and health and by using two different scanners. Also in this study the method performed well with coefficient of variability ranging from 1.4 - 8.8 %.
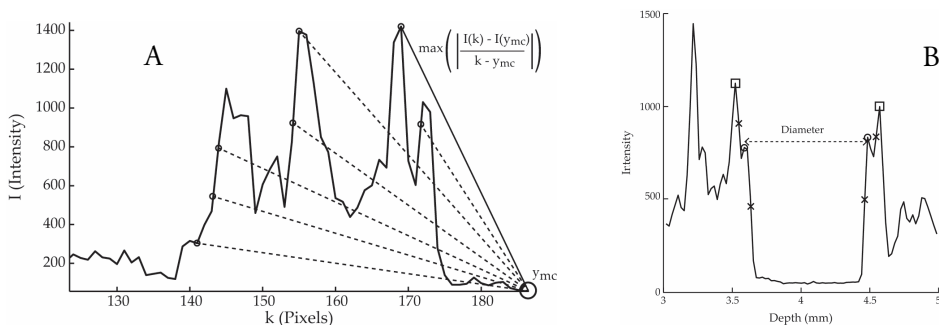
Figure IV. A) Schematic of the initial wall detection algorithm. The position of the wall is determined as the pixel having the maximum slope relative to the location of the mouse click, y_{mc}, in the center of the lumen. B) Averaged intensity profile of the arterial wall. The edges of the intima and adventitia echo, respectively, at the near and far wall are marked with crosses. Peak intensities of the adventitia echo at the near and far wall are marked with squares. Peak intensities of the intima echo at the near and far wall are marked with circles. Lumen diameter at diastole, distension and intima-media thickness were determined.

5.5   Paper VI – overview

The pulsatile blood flow causes a radial distension of the arterial wall. However besides an increase in diameter during the systolic phase there is also a decrease in thickness. This intima-media compression (IMC) is only barely visible for the eye and is quite difficult to measure. However, the IMC might be of importance in cardiovascular research since this is the main site for atherosclerotic manifestation. The aim of this paper was to develop a method that could measure this change in thickness with a reasonable repeatability.

The key feature of the developed method is that there is a measure of and a compensation for the longitudinal movement. In ultrasound images there are often irregularities in the arterial wall. This results in a somewhat "wavy" appearance to the different layers of the arterial wall (Fig. VI-A). Therefore the automatically measured intima-media thickness (IMT) varies (falsely) depending on where on these "waves" it is measured.

The average IMT for all (image) lines was measured in the first frame. Then the idea was to increase the accuracy by keeping track of the longitudinal movement for both the intima-media complex and the adventitia, using the sum of absolute difference. The IMT measured for each line in one frame could then be compared to the thickness measured between the *same* physical locations in each layer separately in the next frame. The mean *difference* in IMT for all locations is then independent of the individually measured IMT. The IMT during all frames was then determined as a cumulative sum starting with the mean IMT of the first frame (Fig. VI-B). The mean IMC (total compression, Fig. VI-B) was 66 µm (9.2%) measured with a coefficient of variability of 9.9%.
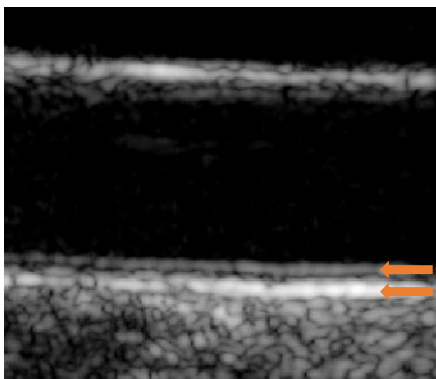
Figure VI-A. A typical ultrasound image of the common carotid artery. The echoes originating from the intima and adventitial layers of the arterial wall form a typical double-line pattern as indicated by the arrows. Notice the "wavy" appearance of these lines.
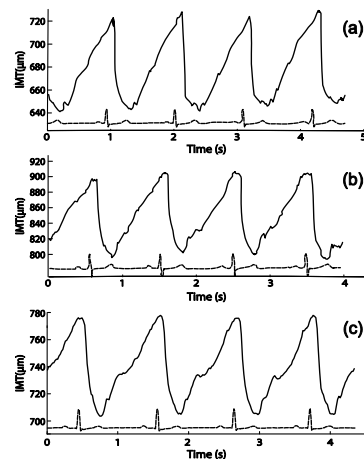

Figure VI-B. The IMT during four cardiac cycle of (a) a health 42 year old female, (b) a healthy 47 year old female and (c) a healthy 49-year old male. The bottom lines shows the ECG.

5.6   Paper VII – overview

As has been previously shown the longitudinal movement of the arterial wall is greater in the innermost layers, the intima-media complex, compared to the outer layer, the adventitia, and the surrounding tissue. During close visual review of several different recordings of carotid arteries a continuous decrease in magnitude of the longitudinal movement was often noticed. The aim of this paper was to measure this continuous change in magnitude.

The method developed for this purpose had two main tasks a) to automatically locate the arterial wall and the angle of it and b) measure the longitudinal movement in small steps perpendicular to the blood flow. The second task requires a very small axial length of the ROI thus substantially increasing the risk for detecting false axial motions. Therefore the first task was also required, the localization and angle determination of the arterial wall. The position of the wall could then be used to axially lock the ROI and the search was performed in only one direction.

To increase the sub-pixel accuracy beyond the size of individual pixels the peaks of the horizontal amplitude were identified by locating the zero-crossings using the equation of a straight line (Fig. VII-A). These peak positions were then matched to those in the previous frame, indirectly yielding the inter-frame longitudinal movement. This was then repeated while moving the ROI throughout the arterial wall. As expected the maximum shear strain was shown to occur between the media and adventitia (Fig. VII-B).

Figure VII-B. The maximum measured longitudinal displacement at different depth within the common carotid artery of a healthy 49-year-old female. The area with maximum shear strain is indicated by the arrow.

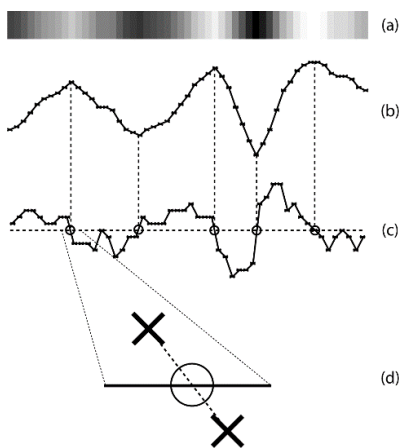Figure VII-A. Schematic illustration of the peaks in the B-mode image and the corresponding zero-crossings in the differentiated data. A horizontal B-mode line of the arterial wall (a) can be represented as an intensity curve (b). The zero-crossings of the differentiated intensity curve (c) correspond to the local peaks. Sub-pixel accuracy is obtained using the equation of straight lines at each zero-crossing (d).
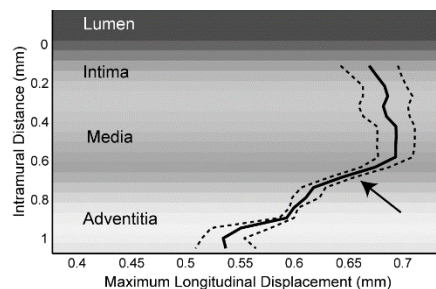
6. REFERENCES

1.   Global status report on noncommunicable diseases 2010. *World Health Organization*. 2011.
2.   Ross R. Mechanisms of disease: Atherosclerosis — an inflammatory disease. *N. Engl. J. Med.* 1999;340:115-126.
3.   Nichols WW, O'Rourke MF, Vlachopoulos C. Mcdonald's blood flow in arteries : Theoretical, experimental and clinical principles. 2011.
4.   Yusuf S, Hawken S, Ounpuu S, Dans T, Avezum A, Lanas F, McQueen M, Budaj A, Pais P, Varigos J, Liu LS, Investigators IS. Effect of potentially modifiable risk factors associated with myocardial infarction in 52 countries (the interheart study): Case-control study. *Lancet*. 2004;364:937-952.
5.   Mcmillan DE. Blood-flow and the localization of atherosclerotic plaques. *Stroke*. 1985;16:582-587.
6.   Lin MC, AlmusJacobs F, Chen HH, Parry GCN, Mackman N, Shyy JYJ, Chien S. Shear stress induction of the tissue factor gene. *J Clin Invest*. 1997;99:737-744.
7.   Mondy JS, Lindner V, Miyashiro JK, Berk BC, Dean RH, Geary RL. Platelet-derived growth factor ligand and receptor expression in response to altered blood flow in vivo. *Circulation Research*. 1997;81:320-327.
8.   Nakashima Y, Raines EW, Plump AS, Breslow JL, Ross R. Upregulation of vcam-1 and icam-1 at atherosclerosis-prone sites on the endothelium in the apoe-deficient mouse. *Arterioscl Throm Vas*. 1998;18:842-851.
9.   Heidenreich PA, Trogdon JG, Khavjou OA, Butler J, Dracup K, Ezekowitz MD, Finkelstein EA, Hong YL, Johnston SC, Khera A, Lloyd-Jones DM, Nelson SA, Nichol G, Orenstein D, Wilson PWF, Woo YJ, Coordina AHAA, Council S, Inter CCR, Cardiology CC, Prevention CE, Thrombosi CA, C CCC, Nursing CC, Dis CKC, Anesthe CCS, Quality IC. Forecasting the future of cardiovascular disease in the united states a policy statement from the american heart association. *Circulation*. 2011;123:933-944.
10.   Berglund E, Jönsson BA. *Medicinsk fysik*. Studentlitteratur; 2007.
11.   ten Kate GL, Sijbrands EJ, Staub D, Coll B, ten Cate FJ, Feinstein SB, Schinkel AFL. Noninvasive imaging of the vulnerable atherosclerotic plaque. *Curr Prob Cardiology*. 2010;35:556-591.
12.   Loizou CP. A review of ultrasound common carotid artery image and video segmentation techniques. *Med Biol Eng Comput*. 2014;52:1073-1093.
13.   Arndt JO, Klauske J, Mersch F. Diameter of intact carotid artery in man and its change with pulse pressure. *Pflug Arch Eur J Phy*. 1968;301:230-240.

14.   Hokanson DE, Strandne.De, Sumner DS, Mozersky DJ. Phase-locked echo tracking system for recording arterial diameter changes in-vivo. *J Appl Physiol*. 1972;32:728-733.

15.   Cinthio M, Jansson T, Eriksson A, Ahlgren AR, Persson HW, Lindstrom K. Evaluation of an algorithm for arterial lumen diameter measurements by means of ultrasound. *Med Biol Eng Comput*. 2010;48:1133-1140.

16.   Cinthio M, Jansson T, Ahlgren AR, Lindstrom K, Persson HW. A method for arterial diameter change measurements using ultrasonic b-mode data. *Ultrasound Med Biol*. 2010;36:1504-1512.

17.   Hoeks APG, Ruissen CJ, Hick P, Reneman RS. Trans-cutaneous detection of relative changes in artery diameter. *Ultrasound Med Biol*. 1985;11:51-59.

18.   Tortoli P, Bettarini R, Guidi F, Andreuccetti F, Righi D. A simplified approach for real-time detection of arterial wall velocity and distension. *IEEE Trans. Ultrason. Ferroelect. Freq. Contr.* 2001;48:1005-1012.

19.   Khamdaeng T, Luo J, Vappou J, Terdtoon P, Konofagou EE. Arterial stiffness identification of the human carotid artery using the stress-strain relationship in vivo. *Ultrasonics*. 2012;52:402-411.

20.   Pignoli P, Tremoli E, Poli A, Oreste P, Paoletti R. Intimal plus medial thickness of the arterial-wall - a direct measurement with ultrasound imaging. *Circulation*. 1986;74:1399-1406.

21.   Liang Q, Wendelhag I, Wikstrand J, Gustavsson T. A multiscale dynamic programming procedure for boundary detection in ultrasonic artery images. *IEEE Trans. Med. Imaging*. 2000;19:127-142.

22.   Golemati S, Stoitsis J, Sifakis EG, Balkizas T, Nikita KS. Using the hough transform to segment ultrasound images of longitudinal and transverse sections of the carotid artery. *Ultrasound Med Biol*. 2007;33:1918-1932.

23.   Loizou CP, Pattichis CS, Pantziaris M, Tyllis T, Nicolaides A. Snakes based segmentation of the common carotid artery intima media. *Med Biol Eng Comput*. 2007;45:35-49.

24.   Molinari F, Zeng G, Suri JS. A state of the art review on intima-media thickness (imt) measurement and wall segmentation techniques for carotid ultrasound. *Comput Meth Prog Bio*. 2010;100:201-221.

25.   Naik V, Gamad RS, Bansod PP. Carotid artery segmentation in ultrasound images and measurement of intima-media thickness. *Biomed Res Int*. 2013

26.   Ilea DE, Duffy C, Kavanagh L, Stanton A, Whelan PF. Fully automated segmentation and tracking of the intima media thickness in ultrasound video sequences of the common carotid artery. *IEEE Trans. Ultrason. Ferroelect. Freq. Contr.* 2013;60:158-177.

27.   Faita F, Gernignani V, Bianchini ET, Giannarelli C, Ghiadoni L, Demi M. Real-time measurement system for evaluation of the carotid intima-media thickness with a robust edge operator. *J Ultras Med*. 2008;27:1353-1361.

28.	van den Oord SC, Sijbrands EJ, ten Kate GL, van Klaveren D, van Domburg RT, van der Steen AF, Schinkel AF. Carotid intima-media thickness for cardiovascular risk assessment: Systematic review and meta-analysis. *Atherosclerosis*. 2013;228:1-11.

29.	Lawton RW, Greene LC. A method for the *in situ* study of aortic elasticity in the dog. *Authorized Medical Allowance List, US Naval and Air Development Center*. NADC-MA-5603. 1956.

30.	Patel DJ, Mallos AJ, Fry DL. Aortic mechanics in the living dog. *J Applied Physiology*. 1961;16:293-299.

31.	Patel DJ, Fry DL. The elastic symmetry of arterial segments in dogs. *Circ Res*. 1969;24:1-8.

32.	Deng SX, Tomioka J, Debes JC, Fung YC. New experiments on shear modulus of elasticity of arteries. *Am J Physiol Heart Circ Physiol*. 1994;266:H1-H10.

33.	Tozzi P, Hayoz D, Oedman C, Mallabiabarrena I, von Segesser LK. Systolic axial artery length reduction: An overlooked phenomenon *in vivo*. *Am J Physiol Heart Circ Physiol*. 2001;280:H2300-H2305.

34.	Persson M, Rydén Ahlgren Å, Jansson T, Eriksson A, Persson HW, Lindström K. A new non-invasive ultrasonic method for simultaneous measurements of longitudinal and radial arterial wall movements: First *in vivo* trial. *Clin. Physiol. Funct. Imaging*. 2003;23:247-251.

35.	Cinthio M, Ahlgren ÅR, Jansson T, Eriksson A, Persson HW, Lindström K. Evaluation of an ultrasonic echo-tracking method for measurements of arterial wall movements in two dimensions. *IEEE Trans Ultrason Ferroelect Freq Contr*. 2005;52:1300-1311.

36.	Cinthio M, Ahlgren AR, Bergkvist J, Jansson T, Persson HW, Lindstrom K. Longitudinal movements and resulting shear strain of the arterial wall. *Am J Physiol-Heart C*. 2006;291:H394-H402.

37.	Ahlgren ÅR, Cinthio M, Steen S, Persson HW, Sjöberg T, Lindström K. Effects of adrenaline on longitudinal arterial wall movements and resulting intramural shear strain: A first report. *Clin Physiol Funct Imaging*. 2009;29:353-359.

38.	Ahlgren ÅR, Cinthio M, Steen S, Nilsson T, Sjöberg T, Persson HW, Lindström K. Longitudinal displacement and intramural shear strain of the porcine carotid artery undergo profound changes in response to catecholamines. *Am. J. Physiol. Heart. Circ. Physiol*. 2012;302:H1102-H1115.

39.	Ahlgren AR, Steen S, Segstedt S, Erlov T, Lindstrom K, Sjoberg T, Persson HW, Ricci S, Tortoli P, Cinthio M. Profound increase in longitudinal displacements of the porcine carotid artery wall can take place independently of wall shear stress: A continuation report. *Ultrasound Med Biol*. 2015;41:1342-1353.

40. Warriner RK, Johnston KW, Cobbold RSC. A viscoelastic model of arterial wall motion in pulsatile flow: Implications for doppler ultrasound clutter assessment. *Physiol Meas*. 2008;29:157-179.

41. Golemati S, Sassano A, Lever MJ, Bharath AA, Dhanjil S, Nicolaides AN. Carotid artery wall motion estimated from b-mode ultrasound using region tracking and block matching. *Ultrasound Med Biol*. 2003;29:387-399.

42. Zahnd G, Boussel L, Marion A, Durand M, Moulin P, Serusclat A, Vray D. Measurement of two-dimensional movement parameters of the carotid artery wall for early detection of arteriosclerosis: A preliminary clinical study. *Ultrasound Med Biol*. 2011;37:1421-1429.

43. Zahnd G, Vray D, Serusclat A, Alibay D, Bartold M, Brown A, Durand M, Jamieson LM, Kapellas K, Maple-Brown LJ, O'Dea K, Moulin P, Celermajer DS, Skilton MR. Longitudinal displacement of the carotid wall and cardiovascular risk factors: Associations with aging, adiposity, blood pressure and periodontal disease independent of cross-sectional distensibility and intima-media thickness. *Ultrasound Med Biol*. 2012;38:1705-1715.

44. Zahnd G, Orkisz M, Serusclat A, Moulin P, Vray D. Evaluation of a kalman-based block matching method to assess the bi-dimensional motion of the carotid artery wall in b-mode ultrasound sequences. *Med Image Anal*. 2013;17:573-585.

45. Svedlund S, Eklund C, Robertsson P, Lomsky M, Gan LM. Carotid artery longitudinal displacement predicts 1-year cardiovascular outcome in patients with suspected coronary artery disease. *Arterioscl Throm Vas*. 2011;31:1668-1674.

46. Lehmann ED, Hopkins KD, Rawesh A, Joseph RC, Kongola K, Coppack SW, Gosling RG. Relation between number of cardiovascular risk factors/events and noninvasive doppler ultrasound assessments of aortic compliance. *Hypertension*. 1998;32:565-569.

47. Laurent S, Boutouyrie P, Asmar R, Gautier I, Laloux B, Guize L, Ducimetiere P, Benetos A. Aortic stiffness is an independent predictor of all-cause and cardiovascular mortality in hypertensive patients. *Hypertension*. 2001;37:1236-1241.

48. Boutouyrie P, Tropeano AI, Asmar R, Gautier I, Benetos A, Lacolley P, Laurent S. Aortic stiffness is an independent predictor of primary coronary events in hypertensive patients - a longitudinal study. *Hypertension*. 2002;39:10-15.

49. Lehmann ED, Hopkins KD, Gosling RG. Direct aortic distensibility measurements and their reproductibility. *Eur Heart J*. 1994;15:1441-1442.

50. Avolio AP, Chen SG, Wang RP, Zhang CL, Li MF, Orourke MF. Effects of aging on changing arterial compliance and left-ventricular load in a northern chinese urban-community. *Circulation*. 1983;68:50-58.

51.   Laurent S, Cockcroft J, Van Bortel L, Boutouyrie P, Giannattasio C, Hayoz D, Pannier B, Vlachopoulos C, Wilkinson I, Struijker-Boudier H, Non-invasive EN. Expert consensus document on arterial stiffness: Methodological issues and clinical applications. *Eur Heart J.* 2006;27:2588-2605.

52.   Asmar R, Benetos A, Topouchian J, Laurent P, Pannier B, Brisac AM, Target R, Levy BI. Assessment of arterial distensibility by automatic pulse-wave velocity-measurement - validation and clinical-application studies. *Hypertension.* 1995;26:485-490.

53.   Karamanoglu M. Errors in estimating propagation distances in pulse wave velocity. *Hypertension.* 2003;41:E8-E8.

54.   Xu JP. Do we need a better approach for measuring pulse-wave velocity? *Ultrasound Med Biol.* 2003;29:1373-1373.

55.   Benthin M, Dahl P, Ruzicka R, Lindstrom K. Calculation of pulse-wave velocity using cross-correlation - effects of reflexes in the arterial tree. *Ultrasound Med Biol.* 1991;17:461-469.

56.   Brands PJ, Willigers JM, Ledoux LAF, Reneman RS, Hoeks APG. A noninvasive method to estimate pulse wave velocity in arteries locally by means of ultrasound. *Ultrasound Med Biol.* 1998;24:1325-1335.

57.   Meinders JM, Kornet L, Brands PJ, Hoeks APG. Assessment of local pulse wave velocity in arteries using 2d distension waveforms. *Ultrasonic imaging.* 2001;23:199-215.

58.   Eriksson A, Greiff E, Loupas T, Persson M, Pesque P. Arterial pulse wave velocity with tissue doppler imaging. *Ultrasound Med Biol.* 2002;28:571-580.

59.   Rabben SI, Stergiopulos N, Hellevik LR, Smiseth OA, Slordahl S, Urheim S, Angelsen B. An ultrasound-based method for determining pulse wave velocity in superficial arteries. *J Biomech.* 2004;37:1615-1622.

60.   Bramwell JC. The velocity of the pulse wave in man. *P R Soc Lond B-Conta.* 1922;93:298-306.

61.   Williams R, Needles A, Cherin E, Zhou YQ, Henkelman RM, Adamson SL, Foster FS. Noninvasive ultrasonic measurement of regional and local pulse-wave velocity in mice. *Ultrasound Med Biol.* 2007;33:1368-1375.

62.   Pernot M, Fujikura K, Fung-Kee-Fung SD, Konofagou EE. Ecg-gated, mechanical and electromechanical wave imaging of cardiovascular tissues in vivo. *Ultrasound Med Biol.* 2007;33:1075-1085.

63.   Luo JW, Fujikura K, Tyrie LS, Tilson MD, Konofagou EE. Pulse wave imaging of normal and aneurysmal abdominal aortas in vivo. *IEEE Trans. Med. Imaging.* 2009;28:477-486.

64.   Nandlall SD, Goldklang MP, Kalashian A, Dangra NA, D'Armiento JM, Konofagou EE. Monitoring and staging abdominal aortic aneurysm disease with pulse wave imaging. *Ultrasound Med Biol.* 2014;40:2404-2414.

65.   Fujikura K, Luo JW, Gamarnik V, Pernot M, Fukumoto R, Tilson MD, Konofagou EE. A novel noninvasive technique for pulse-wave imaging and

characterization of clinically-significant vascular mechanical properties in vivo. *Ultrasonic imaging*. 2007;29:137-154.

66. Vappou J, Luo JW, Konofagou EE. Pulse wave imaging for noninvasive and quantitative measurement of arterial stiffness in vivo. *Am J Hypertens*. 2010;23:393-398.

67. Li RX, Luo JW, Balaram SK, Chaudhry FA, Shahmirzadi D, Konofagou EE. Pulse wave imaging in normal, hypertensive and aneurysmal human aortas in vivo: A feasibility study. *Phys Med Biol*. 2013;58:4549-4562.

68. Luo JW, Li RX, Konofagou EE. Pulse wave imaging of the human carotid artery: An in vivo feasibility study. *IEEE Trans. Ultrason. Ferroelect. Freq. Contr.* 2012;59:174-181.

69. Simova I, Katova T, Santoro C, Galderisi M. Comparison between regional and local pulse-wave velocity data. *Echocardiography*. 2015:doi: 10.1111/echo.12985.

70. Naghavi M, Libby P, Falk E, Casscells SW, Litovsky S, Rumberger J, Badimon JJ, Stefanadis C, Moreno P, Pasterkamp G, Fayad Z, Stone PH, Waxman S, Raggi P, Madjid M, Zarrabi A, Burke A, Yuan C, Fitzgerald PJ, Siscovick DS, de Korte CL, Aikawa M, Airaksinen KEJ, Assmann G, Becker CR, Chesebro JH, Farb A, Galis ZS, Jackson C, Jang IK, Koenig W, Lodder RA, March K, Demirovic J, Navab M, Priori SG, Rekhter MD, Bahr R, Grundy SM, Mehran R, Colombo A, Boerwinkle E, Ballantyne C, Insull W, Schwartz RS, Vogel R, Serruys PW, Hansson GK, Faxon DP, Kaul S, Drexler H, Greenland P, Muller JE, Virmani R, Ridker PM, Zipes DP, Shah PK, Willerson JT. From vulnerable plaque to vulnerable patient - a call for new definitions and risk assessment strategies: Part i. *Circulation*. 2003;108:1664-1672.

71. Ophir J, Cespedes I, Ponnekanti H, Yazdi Y, Li X. Elastography - a quantitative method for imaging the elasticity of biological tissues. *Ultrasonic imaging*. 1991;13:111-134.

72. Bonnefous O, Brevannes L, Denis E, Sananes JC, Montaudon M, Laurent FH, Drouillard J. New noninvasive echographic technique for arterial wall characterization. *Radiology*. 1996;201:1129-1129.

73. Kanai H, Sato M, Koiwa Y, Chubachi N. Transcutaneous measurement and spectrum analysis of heart wall vibrations. *IEEE Trans. Ultrason. Ferroelect. Freq. Contr.* 1996;43:791-810.

74. Kanai H, Hasegawa H, Chubachi N, Koiwa Y, Tanaka M. Noninvasive evaluation of local myocardial thickening and its color-coded imaging. *IEEE Trans. Ultrason. Ferroelect. Freq. Contr.* 1997:752-768.

75. Hasegawa H, Kanai H. Reduction of influence of variation in center frequencies of rf echoes on estimation of artery-wall strain. *IEEE Trans. Ultrason. Ferroelect. Freq. Contr.* 2008;55:1921-1934.

76. Kanai H, Hasegawa H, Ichiki M, Tezuka F, Koiwa Y. Elasticity imaging of atheroma with transcutaneous ultrasound preliminary study. *Circulation*. 2003;107:3018-3021.

77. Okimoto H, Ishigaki Y, Koiwa Y, Hinokio Y, Ogihara T, Suzuki S, Katagiri H, Ohkubo T, Hasegawa H, Kanai H, Oka Y. A novel method for evaluating human carotid artery elasticity: Possible detection of early stage atherosclerosis in subjects with type 2 diabetes. *Atherosclerosis*. 2008;196:391-397.

78. Tokita A, Ishigaki Y, Okimoto H, Hasegawa H, Koiwa Y, Kato M, Ishihara H, Hinokio Y, Katagiri H, Kanai H, Oka Y. Carotid arterial elasticity is a sensitive atherosclerosis value reflecting visceral fat accumulation in obese subjects. *Atherosclerosis*. 2009;206:168-172.

79. Shi H, Mitchell CC, McCormick M, Kliewer MA, Dempsey RJ, Varghese T. Preliminary in vivo atherosclerotic carotid plaque characterization using the accumulated axial strain and relative lateral shift strain indices. *Phys Med Biol*. 2008;53:6377-6394.

80. Maurice RL, Bertrand R. Lagrangian speckle model and tissue-motion estimation - theory. *IEEE Trans. Med. Imaging*. 1999;18:593-603.

81. Maurice RL, Ohayon J, Fretigny Y, Bertrand M, Soulez G, Cloutier G. Noninvasive vascular elastography: Theoretical framework. *IEEE Trans. Med. Imaging*. 2004;23:164-180.

82. Maurice RL, Soulez G, Giroux M-F, Cloutier G. Noninvasive vascular elastography for carotid artery characterization on subjects without previous history of atherosclerosis. *Medical physics*. 2008;35:3436-3443.

83. Larsson M, Heyde B, Kremer F, Brodin LA, D'hooge J. Ultrasound speckle tracking for radial, longitudinal and circumferential strain estimation of the carotid artery - an in vitro validation via sonomicrometry using clinical and high-frequency ultrasound. *Ultrasonics*. 2015;56:399-408.

84. Widman E, Caidahl K, Heyde B, D'hooge J, Larsson M. Ultrasound speckle tracking strain estimation of in vivo carotid artery plaque with in vitro sonomicrometry validation. *Ultrasound Med Biol*. 2015;41:77-88.

85. Schaar JA, de Korte CL, Mastik F, Strijder C, Pasterkamp G, Boersma E, Serruys PW, van der Steen AFW. Characterizing vulnerable plaque features with intravascular elastography. *Circulation*. 2003;108:2636-2641.

86. de Korte CL, van der Steen AFW, Cespedes EI, Pasterkamp G. Intravascular ultrasound elastography in human arteries: Initial experience in vitro. *Ultrasound Med Biol*. 1998;24:401-408.

87. de Korte CL, Sierevogel MJ, Mastik F, Strijder C, Schaar JA, Velema E, Pasterkamp G, Serruys PW, van der Steen AF. Identification of atherosclerotic plaque components with intravascular ultrasound elastography in vivo: A yucatan pig study. *Circulation*. 2002;105:1627-1630.

88. Hansen HH, Saris AE, Vaka NR, Nillesen MM, de Korte CL. Ultrafast vascular strain compounding using plane wave transmission. *J Biomech*. 2014;47:815-823.

89. Jensen JA, Svendsen NB. Calculation of pressure fields from arbitrarily shaped, apodized, and excited ultrasound transducers. *IEEE Trans. Ultrason. Ferroelect. Freq. Contr.* 1992;39:262-267.

90. Jensen JA. Field: A program for simulating ultrasound systems. *Medical and Biological Engineering and Computing*. 1996;34:351-352.

91. Widman E, Maksuti E, Larsson D, Urban MW, Bjallmark A, Larsson M. Shear wave elastography plaque characterization with mechanical testing validation: A phantom study. *Phys Med Biol*. 2015;60:3151-3174.

92. Ramnarine KV, Garrard JW, Dexter K, Nduwayo S, Panerai RB, Robinson TG. Shear wave elastography assessment of carotid plaque stiffness: In vitro reproducibility study. *Ultrasound Med Biol*. 2014;40:200-209.

93. Ramnarine KV, Garrard JW, Kanber B, Nduwayo S, Hartshorne TC, Robinson TG. Shear wave elastography imaging of carotid plaques: Feasible, reproducible and of clinical potential. *Cardiovascular Ultrasound*. 2014;12

94. Sarvazyan A, Hall TJ, Urban MW, Fatemi M, Aglyamov SR, Garra BS. An overview of elastography-an emerging branch of medical imaging. *Curr Med Imaging Rev*. 2011;7:255-282.

95. Tatar IG, Kurt A, Hekimoglu B. Ultrasound elastography: A new era for vulnerable carotid plaque imaging? *J. Card. Surg.* 2013;1:20-24.

96. ElBarghouty NM, Levine T, Ladva S, Flanagan A, Nicolaides A. Histological verification of computerised carotid plaque characterisation. *Eur J Vasc Endovasc*. 1996;11:414-416.

97. Wilhjelm JE, Gronholdt MLM, Wiebe B, Jespersen SK, Hansen LK, Sillesen H. Quantitative analysis of ultrasound b-mode images of carotid atherosclerotic plaque: Correlation with visual classification and histological examination. *IEEE Trans. Med. Imaging*. 1998;17:910-922.

98. Vince DG, Dixon KJ, Cothren RM, Cornhill JF. Comparison of texture analysis methods for the characterization of coronary plaques in intravascular ultrasound images. *Computerized Medical Imaging and Graphics*. 2000;24:221-229.

99. Haralick RM, Shanmuga.K, Dinstein I. Textural features for image classification. *IEEE Trans. Syst. Man Cyb*. 1973;Smc3:610-621.

100. Tsiaparas NN, Golemati S, Andreadis I, Stoitsis JS, Valavanis I, Nikita KS. Comparison of multiresolution features for texture classification of carotid atherosclerosis from b-mode ultrasound. *IEEE Trans. Inf. Technol. B*. 2011;15:130-137.

101. Kakkos SK, Nicolaides AN, Kyriacou E, Daskalopoulou SS, Sabetai MM, Pattichis CS, Geroulakos G, Griffin MB, Thomas D. Computerized texture analysis of carotid plaque ultrasonic images can identify unstable plaques

associated with ipsilateral neurological symptoms. *Angiology*. 2011;62:317-328.

102. Kuc R, Schwartz M. Estimating the acoustic attenuation coefficient slope for liver from reflected ultrasound signals. *IEEE Trans. Son. Ultrason.* 1979;26:353-362.

103. Fink M, Hottier F, Cardoso JF. Ultrasonic signal-processing for invivo attenuation measurement - short-time fourier-analysis. *Ultrasonic imaging*. 1983;5:117-135.

104. Flax SW, Pelc NJ, Glover GH, Gutmann FD, Mclachlan M. Spectral characterization and attenuation measurements in ultrasound. *Ultrasonic imaging*. 1983;5:95-116.

105. Picano E, Landini L, Distante A, Benassi A, Sarnelli R, L'Abbate A. Fibrosis, lipids, and calcium in human atherosclerotic plaque. In vitro differentiation from normal aortic walls by ultrasonic attenuation. *Circulation research*. 1985;56:556.

106. Shi HR, Tu HF, Dempsey RJ, Varghese T. Ultrasonic attenuation estimation in small plaque samples using a power difference method. *Ultrasonic imaging*. 2007;29:15-30.

107. Nam K, Rosado-Mendez IM, Wirtzfeld LA, Ghoshal G, Pawlicki AD, Madsen EL, Lavarello RJ, Oelze ML, Zagzebski JA, O'Brien WD, Hall TJ. Comparison of ultrasound attenuation and backscatter estimates in layered tissue-mimicking phantoms among three clinical scanners. *Ultrasonic imaging*. 2012;34:209-221.

108. Madsen EL, Insana MF, Zagzebski JA. Method of data reduction for accurate determination of acoustic backscatter coefficients. *J Acoust Soc Am*. 1984;76:913-923.

109. Yao LX, Zagzebski JA, Madsen EL. Backscatter coefficient measurements using a reference phantom to extract depth-dependent instrumentation factors. *Ultrasonic imaging*. 1990;12:58-70.

110. Labyed Y, Bigelow TA. A theoretical comparison of attenuation measurement techniques from backscattered ultrasound echoes. *J Acoust Soc Am*. 2011;129:2316-2324.

111. Morse PM, Ingard KU. *Theoretical acoustics*. McGraw-Hill, New York; 1968.

112. Lizzi FL, Greenebaum M, Feleppa EJ, Elbaum M, Coleman DJ. Theoretical framework for spectrum analysis in ultrasonic tissue characterization. *J Acoust Soc Am*. 1983;73:1366-1373.

113. Lizzi FL, Ostromogilsky M, Feleppa EJ, Rorke MC, Yaremko MM. Relationship of ultrasonic spectral parameters to features of tissue microstructure. *IEEE Trans. Ultrason. Ferroelect. Freq. Contr.* 1987;34:319-329.

114. Insana MF, Wagner RF, Brown DG, Hall TJ. Describing small-scale structure in random-media using pulse-echo ultrasound. *J Acoust Soc Am*. 1990;87:179-192.

115. Faran JJ. Sound scattering by solid cylinders and spheres. *J Acoust Soc Am*. 1951;23:405-418.

116. Insana MF, Hall TJ. Parametric ultrasound imaging from backscatter coefficient measurements - image-formation and interpretation. *Ultrasonic imaging*. 1990;12:245-267.

117. Feleppa EJ, Lizzi FL, Coleman DJ, Yaremko MM. Diagnostic spectrum analysis in ophthalmology - a physical perspective. *Ultrasound Med Biol*. 1986;12:623-631.

118. Oelze ML, Zachary JF. Characterization of tissue microstructure using ultrasonic backscatter: Theory and technique for optimization using a gaussian form factor. *J Acoust Soc Am*. 2002;112:1202-1211.

119. Sannachi L, Tadayyon H, Sadeghi-Naini A, Tran W, Gandhi S, Wright F, Oelze M, Czarnota G. Non-invasive evaluation of breast cancer response to chemotherapy using quantitative ultrasonic backscatter parameters. *Med Image Anal*. 2015;20:224-236.

120. Noritomi T, Sigel B, Swami V, Justin J, Gahtan V, Chen X, Feleppa EJ, Roberts AB, Shirouzu K. Carotid plaque typing by multiple-parameter ultrasonic tissue characterization. *Ultrasound in Medicine & Biology*. 1997;23:643-650.

121. Bridal SL, Beyssen B, Fornes P, Julia P, Berger G. Multiparametric attenuation and backscatter images for characterization of carotid plaque. *Ultrasonic imaging*. 2000;22:20-34.

122. Waters KR, Bridal SL, Cohen-Bacrie C, Levrier C, Fornes P, Laugier P. Parametric analysis of carotid plaque using a clinical ultrasound imaging system. *Ultrasound Med Biol*. 2003;29:1521-1530.

123. Shi HR, Varghese T, Mitchell CC, McCormick M, Dempsey RJ, Kliewer MA. In vivo attenuation and equivalent scatterer size parameters for atherosclerotic carotid plaque: Preliminary results. *Ultrasonics*. 2009;49:779-785.

124. Yamada K, Yoshimura S, Kawasaki M, Enomoto Y, Asano T, Minatoguchi S, Iwama T. Effects of atorvastatin on carotid atherosclerotic plaques: A randomized trial for quantitative tissue characterization of carotid atherosclerotic plaques with integrated backscatter ultrasound. *Cerebrovasc Dis*. 2009;28:417-424.

125. Nair A, Kuban BD, Obuchowski N, Vince DG. Assessing spectral algorithms to predict atherosclerotic plaque composition with normalized and raw intravascular ultrasound data. *Ultrasound Med Biol*. 2001;27:1319-1331.

126.   Nair A, Kuban BD, Tuzcu EM, Schoenhagen P, Nissen SE, Vince DG. Coronary plaque classification with intravascular ultrasound radiofrequency data analysis. *Circulation*. 2002;106:2200-2206.

127.   Taki A, Hetterich H, Roodaki A, Setarehdan SK, Unal G, Rieber J, Navab N, Konigy A. A new approach for improving coronary plaque component analysis based on intravascular ultrasound images. *Ultrasound Med Biol*. 2010;36:1245-1258.

128.   Kawasaki M, Takatsu H, Noda T, Sano K, Ito Y, Hayakawa K, Tsuchiya K, Arai M, Nishigaki K, Takemura G, Minatoguchi S, Fujiwara T, Fujiwara H. In vivo quantitative tissue characterization of human coronary arterial plaques by use of integrated backscatter intravascular ultrasound and comparison with angioscopic findings. *Circulation*. 2002;105:2487-2492.

129.   Seabra JC, Ciompi F, Pujol O, Mauri J, Radeva P, Sanches J. Rayleigh mixture model for plaque characterization in intravascular ultrasound. *IEEE Trans. Biomed. Eng.* 2011;58:1314-1324.

130.   Katouzian A, Sathyanarayana S, Baseri B, Konofagou EE, Carlier SG. Challenges in atherosclerotic plaque characterization with intravascular ultrasound (ivus): From data collection to classification. *IEEE Trans. Inf. Technol. B*. 2008;12:315-327.

131.   Gerig A, Zagzebski J, Varghese T. Statistics of ultrasonic scatterer size estimation with a reference phantom. *J Acoust Soc Am*. 2003;113:3430-3437.

132.   Boashash B. Estimating and interpreting the instantaneous frequency of a signal .1. Fundamentals. *Proc. IEEE*. 1992;80:520-538.

133.   Gehlbach SM, Sommer FG, Stern RA. Scatterer-induced frequency variations in reflected acoustic pulses: Implications for tissue characterization. *Ultrasonic imaging*. 1985;7:172-178.

134.   Kasai C, Namekawa K, Koyano A, Omoto R. Real-time two-dimensional blood-flow imaging using an auto-correlation technique. *IEEE Trans. Son. Ultrason*. 1985;32:458-464.

135.   Sirmans D, Bumgarner B. Numerical comparison of 5 mean frequency estimators. *J Appl Meteorol*. 1975;14:991-1003.